# Competitive Nucleophilic Attack between Carbon and Metal Atoms in Bridging Hydrocarbyls: X-ray Structures of $Fe_2(CO)_5(\mu\text{-}PPh_2)[\mu\text{-}C{=}C(Ph)PPh_2CH_2PPh_2]$, a Novel Zwitterionic Vinylidene Complex, and $Fe_2(CO)_4(\mu\text{-}PPh_2)(\mu_2\text{-}\eta^2\text{-}C{\equiv}CPr^i)(\mu\text{-}Ph_2PCH_2CH_2PPh_2)$, a Diphosphine-Bridged Acetylide

Andrew A. Cherkas, Simon Doherty, Michael Cleroux, Graeme Hogarth, Leslie H. Randall, Susan M. Breckenridge, Nicholas J. Taylor, and Arthur J. Carty*

*Guelph-Waterloo Centre for Graduate Work in Chemistry, Waterloo Campus, Department of Chemistry, University of Waterloo, Waterloo, Ontario, Canada N2L 3G1*

*Received October 24, 1991*

The $\sigma$–$\pi$ acetylide complex $Fe_2(CO)_6(\mu\text{-}PPh_2)(\mu_2\text{-}\eta^2\text{-}C{\equiv}CPh)$ (**1A**) reacts with the diphosphines bis(diphenylphosphino)methane (dppm) and bis(diphenylphosphino)ethane (dppe) to yield $Fe_2(CO)_5(\mu\text{-}PPh_2)[\mu\text{-}C{=}C(Ph)PPh_2CH_2PPh_2]$ (**2A**) and $Fe_2(CO)_4(\mu\text{-}PPh_2)(\mu_2\text{-}\eta^2\text{-}C{\equiv}CPh)(\mu\text{-dppe})$ (**5A**), respectively. The analogue, $Fe_2(CO)_6(\mu\text{-}PPh_2)(\mu_2\text{-}\eta^2\text{-}C{\equiv}CPr^i)$ (**1B**) reacts with dppm and dppe to yield $Fe_2(CO)_4(\mu\text{-}PPh_2)(\mu_2\text{-}\eta^2\text{-}C{\equiv}CPr^i)(\mu\text{-dppm})$ (**4B**) and $Fe_2(CO)_4(\mu\text{-}PPh_2)(\mu_2\text{-}\eta^2\text{-}C{\equiv}CPr^i)(\mu\text{-dppe})$ (**5B**) while $Fe_2(CO)_6(\mu\text{-}PPh_2)(\mu_2\text{-}\eta^2\text{-}C{\equiv}CBu^t)$ (**1C**) reacts with dppm and dppe to afford $Fe_2(CO)_4(\mu\text{-}PPh_2)(\mu_2\text{-}\eta^2\text{-}C{\equiv}CBu^t)(\mu\text{-dppm})$ (**4C**) and $Fe_2(CO)_4(\mu\text{-}PPh_2)(\mu_2\text{-}\eta^2\text{-}C{\equiv}CBu^t)(\mu\text{-dppe})$ (**5C**). The $\mu$-dppm complex $Fe_2(CO)_4(\mu\text{-}PPh_2)(\mu_2\text{-}\eta^2\text{-}C{\equiv}CPh)(\mu\text{-dppm})$ (**4A**) can also be prepared in high yield from $Fe_2(CO)_6(\mu\text{-CO})(\mu\text{-}Ph_2PCH_2PPh_2)$ and $Ph_2PC{\equiv}CPh$ under UV irradiation and also under prolonged heating of **2A**. The reactions were monitored by $^{31}P$ NMR spectroscopy, allowing the elucidation of mechanistic details. For $Fe_2(CO)_6(\mu\text{-}PPh_2)(\mu_2\text{-}\eta^2\text{-}C{\equiv}CPh)$ (**1A**) both dppm and dppe initially attach at the $\beta$-carbon of the acetylide. For $Fe_2(CO)_6(\mu\text{-}PPh_2)(\mu_2\text{-}\eta^2\text{-}C{\equiv}CBu^t)$ (**1C**) the initial site is the metal, resulting in displacement of carbon monoxide. For $Fe_2(CO)_6(\mu\text{-}PPh_2)(\mu_2\text{-}\eta^2\text{-}C{\equiv}CPr^i)$ (**1B**) both types of intermediate are observed upon reaction with dppe and attack at the $\beta$-carbon of the acetylide predominates for dppm. Complexes **2A** and **5B** have been characterized crystallographically, confirming that the diphosphine moiety is incorporated into a six-membered ring. Complex **2A** has a novel zwitterionic $\mu$-vinylidene ligand formed via nucleophilic attack by one phosphours atom of dppm at the $\beta$-carbon of the acetylide. The remaining phosphorus atom is bound to a metal center. In **5B** the dppe ligand bridges two metal sites. Crystals of **2A** are triclinic, space group $P\bar{1}$, with unit cell dimensions $a$ = 10.438 (1) Å, $b$ = 12.549 (2) Å, $c$ = 21.081 (4) Å, $\alpha$ = 85.07 (2)°, $\beta$ = 79.23 (1)°, and $\gamma$ = 79.63 (1)°. Crystals of **5** are triclinic, space group $P\bar{1}$, with unit cell dimensions $a$ = 10.648 (2) Å, $b$ = 12.888 (2) Å, $c$ = 23.999 (5) Å, $\alpha$ = 77.18 (2)°, $\beta$ = 88.72 (2)°, and $\gamma$ = 69.45 (1)°. The structures were solved and refined to the following $R$ and $R_w$ values; **2A**, $R$ = 0.040 and $R_w$ = 0.048 on 5093 observed ($I > 3\sigma(I)$) data; **5B**, $R$ = 0.054 and $R_w$ = 0.064 on 4195 observed ($I > 3\sigma(I)$) data. In binuclear compounds such as **1A–C**, where the hydrocarbyl is activated by $\sigma$–$\pi$-coordination to two metals, nucleophilic attack at carbon and metal is competitive, with the former more favorable as an initial site.

## Introduction

For polynuclear molecules bearing edge- or face-bridging hydrocarbyl ligands, three common reaction modes toward nucleophiles are observed: direct attack at the organic fragment,[1] ligand substitution,[2] and addition at the metal center with metal–metal bond cleavage.[3] In the specific case of $\mu_2$-$\eta^2$-acetylides with monofunctional nucleophiles, products resulting from both $\alpha$- and $\beta$-attack at the acetylide carbon atoms and carbonyl substitution have been characterized.[4] The chemistry of such hydrocarbyl ligands toward bidentate phosphine compounds has, however, not previously been explored. A prominent feature of the organometallic chemistry of both bis(diphenylphosphino)methane (dppm) and bis(diphenyl-

(1) (a) Deeming, A. J.; Hasso, S. *J. Organomet. Chem.* **1976**, *112*, C39. (b) Beanan, L. R.; Keister, J. B. *Organometallics* **1985**, *4*, 1713. (c) Bassner, S. L.; Morrison, E. P.; Geoffroy, G. L.; Rheingold, A. L. *J. Am. Chem. Soc.* **1986**, *108*, 5358. (d) Muller, J.; Passon, B.; Pickardt, J. *J. Organomet. Chem.* **1982**, *236*, C11. (e) Boyar, E.; Deeming, A. J.; Kabir, S. E. *J. Chem. Soc., Chem. Commun.* **1986**, 577. (f) For a review of nucleophilic attack at hydrocarbyls in binuclear iron complexes, see: Fehlhammer, W. P.; Stolzenberg, H. In *Comprehensive Organometallic Chemistry*; Wilkinson, G., Stone, F. G. A., Abel, W. E., Eds.; Pergamon: Oxford, U.K., 1982; Chapter 31.4, p 513.

(2) (a) Busetto, L.; Jeffery, J. C.; Mills, R. M.; Stone, F. G. A.; Went, M. J.; Woodward, P. *J. Chem. Soc., Dalton Trans.* **1983**, 101. (b) Rimmelin, J.; Jund, R.; Gross, M.; Bohsoun, A. A. *J. Chem. Soc., Dalton Trans.* **1990**, 3189. (c) Moldes, I.; Ros, J.; Yanez, R.; Mathieu, R.; Solans, X.; Font-Burdia, M. *J. Chem. Soc., Dalton Trans.* **1988**, 1417. (d) Bryne, P. G.; Garcia, M. E.; Tran-Huy, N. H.; Jeffrey, J. C.; Stone, F. G. A. *J. Chem. Soc., Dalton Trans.* **1987**, 1243.

(3) (a) Keijsper, J.; Polm, L. H.; Van Koten, G.; Vrieze, K.; Goubitz, K. J.; Stam, C. H. *Organometallics* **1985**, *4*, 1876. (b) Bruce, M. I.; Williams, M. L. *J. Organomet. Chem.* **1985**, *282*, C11. (c) Kwek, K.; Taylor, N. J.; Carty, A. J. *J. Chem. Soc., Chem. Commun.* **1986**, 230.

(4) (a) Seyferth, D.; Hoke, J. B.; Wheeler, D. R. *J. Organomet. Chem.* **1988**, *341*, 421. (b) Nubel, P. O.; Brown, T. L. *Organometallics* **1984**, *3*, 29. (c) Carty, A. J.; Mott, G. N.; Taylor, N. J. *J. Organomet. Chem.* **1981**, *212*, C54. (d) Carty, A. J.; Taylor, N. J.; Smith, W. F.; Lappert, M. F. *J. Chem. Soc., Chem. Commun.* **1978**, 1017. (e) Smith, W. F.; Taylor, N. J.; Carty, A. J. *J. Chem. Soc., Chem. Commun.* **1976**, 896. (f) Wong, Y. S.; Paik, H. N.; Chieh, P. C.; Carty, A. J. *J. Chem. Soc., Chem. Commun.* **1975**, 309. (g) Mott, G. N.; Carty, A. J. *Inorg. Chem.* **1983**, *22*, 2726. (h) Carty, A. J.; Mott, G. N.; Taylor, N. J.; Yule, J. G. *J. Am. Chem. Soc.* **1978**, *100*, 3051. (i) Carty, A. J.; Mott, G. N.; Taylor, N. J. *J. Organomet. Chem.* **1979**, *182*, C69. (j) Carty, A. J.; Taylor, N. J.; Paik, H. N.; Smith, W.; Yule, J. G. *J. Chem. Soc., Chem. Commun.* **1976**, 41. (k) Carty, A. J.; Mott, G. N.; Taylor, N. J.; Ferguson, G.; Khan, M. A.; Roberts, D. J. *J. Organomet. Chem.* **1978**, *149*, 345. (l) Cherkas, A. A.; Mott, G. N.; Granby, R.; MacLaughlin, S. A.; Yule, J. G.; Taylor, N. J.; Carty, A. J. *Organometallics* **1988**, *7*, 1115. (m) Nuccarione, D.; Taylor, N. J.; Carty, A. J. *Organometallics* **1986**, *5*, 1179. (n) Cherkas, A. A.; Randall, L. H.; Taylor, N. J.; Mott, G. N.; Yule, J. E.; Guinamant, J. L.; Carty, A. J. *Organometallics* **1990**, *9*, 1677.

0276-7333/92/2311-1701$03.00/0 

phosphino)ethane (dppe) is their propensity to be incorporated into five-membered rings,[5] a feature which can be attributed to the steric demands of these ligands. Thus, dppe is an excellent chelating ligand whilst dppm has been extensively used for its ability to bind together two metal centers.[5,6] In contrast to the latter, however, examples in which the dppm ligand bridges a metal and a carbon atom are rare, with only one previous example being reported.[6]

During our studies on the fluxionality of the systems characterized by $M_2(CO)_6(\mu\text{-}PPh_2)(\mu_2\text{-}\eta^2\text{-}C{\equiv}CPh)$ (M = Fe, Ru, Os), we have examined the influence of phosphine substitution on the dynamics of the exchange process.[7] These results prompted us to prepare a series of diphosphine-substituted complexes in which the metal atoms were bridged by a bidentate ligand replacing two CO groups. The original objective of CO displacement from two metal centers was achieved, but in the process we discovered that initial attack occurred at a carbon atom of the hydrocarbyl followed by CO substitution at the metal site. Subsequent rearrangement afforded the binuclear bis CO substitution product. In this paper we describe these novel reactions, the characterization of intermediate P–P–C and M–P–P–C complexes, and their transformation to the disubstitution product.

For dppm the intermediate $Fe_2(CO)_5(\mu\text{-}PPh_2)[\mu\text{-}C{=}C(Ph)Ph_2PCH_2PPh_2]$ (**2A**), in which one dppm phosphorus atom has bonded to $C_\beta$ of the acetylide and the second has displaced a carbonyl from Fe(1), has been isolated and fully characterized by spectroscopy and by a single-crystal X-ray analysis. Complex **2A** transforms readily to $Fe_2(CO)_4(\mu\text{-}PPh_2)(\mu_2\text{-}\eta^2\text{-}C{\equiv}CPh)(\mu\text{-dppm})$ (**4A**). Similarly, $Fe_2(CO)_4(\mu\text{-}PPh_2)(\mu_2\text{-}\eta^2\text{-}C{\equiv}CPh)(\mu\text{-dppe})$ (**5A**) was also isolated and characterized spectroscopically. The effect of the hydrocarbyl R group on the substitution mechanism was investigated by reacting both dppm and dppe with $Fe_2(CO)_6(\mu\text{-}PPh_2)(\mu_2\text{-}\eta^2\text{-}C{\equiv}CPr^i)$ and $Fe_2(CO)_6(\mu\text{-}PPh_2)(\mu_2\text{-}\eta^2\text{-}C{\equiv}CBu^t)$ to afford the bridged diphosphine products $Fe_2(CO)_4(\mu\text{-}PPh_2)(\mu_2\text{-}\eta^2\text{-}C{\equiv}CPr^i)(\mu\text{-dppm})$ (**4B**), $Fe_2(CO)_4(\mu\text{-}PPh_2)(\mu_2\text{-}\eta^2\text{-}C{\equiv}CPr^i)(\mu\text{-dppe})$ (**5B**), $Fe_2(CO)_4(\mu\text{-}PPh_2)(\mu_2\text{-}\eta^2\text{-}C{\equiv}CBu^t)(\mu\text{-dppm})$ (**4C**), and $Fe_2(CO)_4(\mu\text{-}PPh_2)(\mu_2\text{-}\eta^2\text{-}C{\equiv}CBu^t)(\mu\text{-dppe})$ (**5C**). All of these compounds were characterized spectroscopically, and the structure of **5B** has been determined crystallographically. The mechanism by which dppm and dppe react with the diiron $\sigma$–$\pi$-acetylide complex was studied using extensive $^{31}P$ NMR experiments. None of these results has been previously communicated.

## Experimental Section

**General Procedures.** Standard Schlenk line techniques were used and manipulations were carried out under a dry dinitrogen atmosphere. Solvents were dried (heptane and toluene over $LiAlH_4$; hexane, THF, and benzene over sodium and benzophenone; methylene chloride over $P_2O_5$), deoxygenated, and distilled before use. Deuteriochloroform and benzene-$d_6$ for the NMR studies were stored over Linde molecular sieves.

Bis(diphenylphosphino)methane and bis(diphenylphosphino)ethane were purchased from Strem Chemical Co. and used without further purification. Infrared spectra were recorded on a Perkin-Elmer 180 or Nicolet-520 FTIR spectrometer as solutions in 0.5-mm matched sodium chloride cells. NMR spectra were measured on Bruker AC-200, AM-250 or AM-500 instruments and chemical shifts are referenced internally to $Me_4Si$ ($^1H$ or $^{13}C$) or externally to 85% $H_3PO_4$ ($^{31}P$). Microanalyses were performed by M-H-W Laboratories, Phoenix, AZ.

**Synthesis and Characterization.** The complexes $Fe_2(CO)_6(\mu\text{-}PPh_2)(\mu_2\text{-}\eta^2\text{-}C{\equiv}CR)$ (R = Ph, $Bu^t$, $Pr^i$) (**1A–C**) were prepared by previously published methods,[8] as was $Fe_2(CO)_6(\mu\text{-}CO)(\mu\text{-dppm})$.[9]

**Preparation of $Fe_2(CO)_5(\mu\text{-}PPh_2)[\mu_2\text{-}C{=}C(Ph)PPh_2CH_2PPh_2]$ (2A).** The complex $Fe_2(CO)_6(\mu\text{-}PPh_2)(\mu_2\text{-}\eta^2\text{-}C{\equiv}CPh)$ (0.10 g, 0.176 mmol) was stirred in toluene (30 mL) with an equimolar amount of dppm (0.0675 g, 0.176 mmol). The temperature was gradually raised to 50 °C, which resulted in the immediate formation of a yellow precipitate. After 30 min at this temperature, the solution was allowed to cool to room temperature. The yellow precipitate was filtered, washed with 3 × 5 mL portions of heptane, and dried in vacuo. The isolated yield of **2** was typically 80–90%. Single crystals suitable for X-ray analysis were grown from methylene chloride/toluene solution.

Anal. Calcd for $C_{50}H_{37}Fe_2O_5P_3$ (**2A**): C, 65.10; H, 4.04. Found: C, 65.00; H, 4.11. IR ($C_6H_{12}$, $\nu$(CO), $cm^{-1}$): 2008 (vs), 1945 (br vs). $^{31}P\{^1H\}$ NMR ($CD_2Cl_2$, 80.13 MHz, $\delta$): 112.6 ($\mu$-$PPh_2$, d, $^4J_{PP}$ = 13.8 Hz), 54.3 (Fe–$PPh_2$, d, $^2J_{PP}$ = 18.1 Hz), 5.9 ($Ph_2P$–C, dd, $^2J_{PP}$ = 18.1 Hz, $^4J_{PP}$ = 13.8 Hz). $^{13}C\{^1H\}$ NMR ($CD_2Cl_2$, 50.3 MHz, $\delta$): 297.2 ($C_\alpha$, ddd, $^2J_{PC}$ = 76.6 Hz, $^2J_{PC}$ = $^3J_{PC}$ = 11.3 Hz), 220.3 (CO, ddd, $^2J_{PC}$ = 16.6 Hz, $^2J_{PC}$ = 4.4 Hz, $^4J_{PC}$ < 1 Hz), 218.9 (CO, dd, $^2J_{PC}$ = 15.1 Hz, $^2J_{PC}$ = 7.9 Hz), 216.5 (CO, d, $^2J_{PC}$ = 2.6 Hz), 142.2–121.3 (phenyl region), 114.1 ($C_\beta$, d, $^1J_{PC}$ = 81.7 Hz), 24.7 ($CH_2$, dd, $^1J_{PC}$ = 67.6 Hz, $^1J_{PC}$ = 12.4 Hz). $^1H$ NMR ($CD_2Cl_2$, 200.13 MHz, $\delta$): 7.55–6.82 (phenyl region, 35 H), 3.45 ($CH_2$, ddd, $^2J_{HH}$ = 13.8 Hz, $^2J_{PH}$ = 10.0 Hz, $^2J_{PH}$ = 6.3 Hz, 1 H), 2.28 ($CH_2$, ddd, $^2J_{HH}$ = 13.8 Hz, $^2J_{PH}$ = 17.8 Hz, $^2J_{PH}$ = 7.8 Hz, 1 H).

**Thermolysis of $Fe_2(CO)_5(\mu\text{-}PPh_2)[\mu\text{-}C{=}C(Ph)PPh_2CH_2PPh_2]$ (2A).** Thermolysis of a toluene solution (100 mL) of **2A** (0.100 g, 0.108 mmol) at 100 °C for 12 h results in a gradual color change from yellow-orange to deep red. Monitoring the solution by IR spectroscopy indicated the slow formation of **4A**. The solution was cooled to room temperature, concentrated to approximately 10 mL, placed on a 10 × 2-cm Florisil column and eluted with $CH_2Cl_2$/hexane. The first band contained **4A** as the product. The solution was concentrated to 5 mL and stored at −10 °C for 24 h. The isolated yield of red crystals was typically 70–80%.

**Attempted Carbonylation of $Fe_2(CO)_4(\mu\text{-}PPh_2)(\mu_2\text{-}\eta^2\text{-}C{\equiv}CPh)(\mu\text{-dppm})$.** A THF solution (50 mL) of **4A** (0.100 g, 0.111 mmol) was purged with carbon monoxide for 2 weeks. During this time IR spectroscopy showed no sign of **2A** or other products.

**Monitoring the Reaction by $^{31}P$ NMR Spectroscopy.** The starting dinuclear complexes $Fe_2(CO)_6(\mu\text{-}PPh_2)(\mu_2\text{-}\eta^2\text{-}C{\equiv}CR)$ (R = Ph, $Pr^i$, $Bu^t$) (**1A–C**) were dissolved in degassed toluene-$d_8$, and an equimolar amount of the bidentate ligand was added. The $^{31}P$ NMR spectra were monitored as a function of time.

**Preparation of $Fe_2(CO)_4(\mu\text{-}PPh_2)(\mu_2\text{-}\eta^2\text{-}C{\equiv}CPh)(\mu\text{-dppm})$ (4A).** A THF solution (170 mL of $Fe_2(CO)_6(\mu\text{-CO})(\mu\text{-dppm})$ (0.427 g, 0.617 mmol) and $Ph_2PC{\equiv}CPh$ (0.194 g, 0.679 mmol) was purged with $N_2$ and irradiated (250 W) for 4 h. A color change from red to orange was observed. The solvent was removed under reduced pressure and the residue extracted as a slurry with $CH_2Cl_2$ (5 mL). The extract was chromatographed on a 10- × 2-cm Florisil column with $CH_2Cl_2$/hexane eluant. Concentration and subsequent cooling (−20 °C) of the major fraction collected afforded 85–90% isolated yield of red crystals.

Anal. Calcd for $C_{50}H_{39}Cl_2Fe_2O_4P_3$ (**4A**): C, 61.35; H, 4.01. Found: C, 61.90; H, 4.12. IR ($C_6H_{12}$, $\nu$(CO), $cm^{-1}$): 1998 (s), 1951 (vs), 1926 (s), 1907 (w, sh). $^{31}P\{^1H\}$ NMR ($CD_2Cl_2$, 80.13 MHz, $\delta$): ($T$ = 299 K) 178.4 ($\mu$-$PPh_2$, t, $^2J_{PP}$ = 114.3 Hz), 58.6 ($\mu$-dppm, d, $^2J_{PP}$ = 114.2 Hz); ($T$ = 188 K) (ABX pattern) 180.2 ($\mu$-$PPh_2$, dd, $^2J_{PP}$ = 134.4 Hz, $^2J_{PP}$ = 90.0 Hz), 60.6 ($\mu$-dppm, $^2J_{PP}$ = 139.4 Hz, $^2J_{PP}$ = 64.5 Hz), 58.4 ($\mu$-dppm, $^2J_{PP}$ = 90.0 Hz, $J_{PP}$ = 64.5

(5) (a) Puddephatt, R. J. *Chem. Soc. Rev.* **1983**, *12*, 99. (b) Balch, A. L. In *Reactivity of Metal-Metal Bonds*; Chisholm, M. L., Ed.; ACS Symposium Series 155; American Chemical Society: Washington, DC, 1981; p 167. (c) Puddephatt, R. J. *Ibid.*, p 197. (d) Sanger, A. R. *J. Chem. Soc., Chem. Commun.* **1975**, 893. (e) Churchill, M. R.; Lashewycz, R. A. *Inorg. Chem.* **1978**, *17*, 1950. (f) Minghetti, G.; Banditelli, G.; Bandini, A. L. *J. Organomet. Chem.* **1977**, *139*, C80.

(6) Hogarth, G.; Knox, S. A. R.; Lloyd, B. R.; Macpherson, K. A.; Morton, D. A. V.; Orpen, A. G. *J. Chem. Soc., Chem. Commun.* **1988**, 360.

(7) Randall, L. H.; Carty, A. J.; Cherkas, A. A.; Taylor, N. J.; Maclaughlin, S. A. Submitted for publication.

(8) Cherkas, A. A.; Randall, L. H.; MacLaughlin, S. A.; Mott, G. N.; Taylor, N. J.; Carty, A. J. *Organometallics* **1988**, *7*, 964.

(9) Cotton, F. A.; Troup, J. M. *J. Am. Chem. Soc.* **1974**, *96*, 4422.

Hz). $^{13}C\{^1H\}$ NMR ($CD_2Cl_2$, 50.3 MHz, $\delta$): 218.1 (CO, dd, $^2J_{PC}$ = 21.9 Hz, $^2J_{PC}$ = 11.5 Hz), 217.6 (CO, dd, $^2J_{PC}$ = 4.5 Hz, $^2J_{PC}$ = 3.2 Hz), 141.4–125.0 (phenyl region), 100.0 ($C_\beta$, d, $^3J_{PC}$ = 9.5 Hz), 83.5 ($C_\alpha$, d, $^2J_{PC}$ = 38 Hz), 39.9 ($CH_2$, t, $^1J_{PC}$ = 20.9 Hz). $^1H$ NMR ($CD_2Cl_2$, 200.13 MHz, $\delta$): 7.81–6.20 (phenyl region, 35 H), 3.72 ($CH_2$, ddt, $^2J_{HH}$ = 13.93 Hz, $^2J_{PH}$ = 11.3 Hz, $^4J_{PH}$ = 4.4 Hz), 2.90 ($CH_{2'}$, dt, $^2J_{HH}$ = 13.93 Hz, $^2J_{PH}$ = 10.0 Hz).

**Preparation of $Fe_2(CO)_4(\mu\text{-}PPh_2)(\mu_2\text{-}\eta^2\text{-}C{\equiv}CPr^i)(\mu\text{-dppm})$ (4B) and $Fe_2(CO)_4(\mu\text{-}PPh_2)(\mu_2\text{-}\eta^2\text{-}C{\equiv}CBu^t)(\mu\text{-dppm})$ (4C).** A toluene solution of $Fe_2(CO)_6(\mu\text{-}PPh_2)(\mu_2\text{-}\eta^2\text{-}C{\equiv}CPr^i)$ (0.100 g, 0.176 mmol) was stirred with an equimolar amount of dppe (0.0696 g, 0.176 mmol) for 10 min, after which time the temperature was raised to 100 °C and the solution was maintained at this temperature for 1 h. The solution was then cooled to room temperature, concentrated to 5 mL and stored at −10 °C for 48 h. The isolated yield of dark red crystals was typically 80–90%. A similar procedure afforded **4C** in 80% yield.

Anal. Calcd for $C_{46}H_{39}Fe_2O_4P_3$ (**4B**): C, 64.18; H, 4.57. Found: C, 64.02; H, 4.74. IR ($C_6H_{12}$, $\nu$(CO), $cm^{-1}$): 1994 (s), 1955 (vs), 1930 (vs), 1911 (m). $^{31}P\{^1H\}$ NMR ($C_6D_6$, 161.8 MHz, $\delta$): 174.8 ($\mu$-$PPh_2$, t, $^2J_{PP}$ = 112.9 Hz), 52.7 ($\mu$-dppm, d, $^2J_{PP}$ = 112.5 Hz). $^{13}C\{^1H\}$ NMR ($CDCl_3$, 62.8 MHz, $\delta$) 218.3 (CO, dd, $^2J_{PC}$ = 22.0 Hz, $^2J_{PC'}$ = 11.0 Hz), 217.7 (CO, d, $^2J_{PC}$ = 9.2 Hz), 142.1–127.0 (phenyl region), 108.8 ($C_\alpha$, dd, $^2J_{PC}$ = 60.9 Hz, $^2J_{PC}$ = 11.7 Hz), 107.0 ($C_\beta$, d, $^3J_{PC}$ = 9.4 Hz), 41.3 ($CH_2$, t, $^1J_{PC}$ = 19.8 Hz), 25.5 (CH–$Pr^i$, s), 22.3 ($CH_3$–$Pr^i$, s). $^1H$ NMR ($CDCl_3$, 250 MHz, $\delta$): 7.67–7.08 (phenyl region), 3.62 ($CH_2$, dd, $^2J_{PH}$ = 23 Hz, $^2J_{HH}$ = 10 Hz), 2.84 ($CH_{2'}$, dd, $^2J_{PH}$ = 23.3 Hz, $^2J_{HH}$ = 10 Hz), 0.47 (CH, sept, $^3J_{HH}$ = 6.6 Hz), 0.05 ($CH_3$, d, $^3J_{HH}$ = 6.6 Hz).

Anal. Calcd for $C_{47}H_{41}Fe_2O_4P_3$ (**4C**): C, 64.53; H, 4.72. Found: C, 64.43; H, 4.76. IR ($C_6H_{12}$, $\nu$(CO), $cm^{-1}$): 1988 (s), 1960 (vs), 1927 (s), 1917 (m). $^{31}P\{^1H\}$ NMR ($CD_2Cl_2$, 101.3 MHz, $\delta$): 180.9 ($\mu$-$PPh_2$, t, $^2J_{PP}$ = 112.3 Hz), 54.3 ($\mu$-dppm, d, $^2J_{PP}$ = 113.4 Hz). $^{13}C\{^1H\}$ NMR ($CDCl_3$, 50.3 MHz, $\delta$): 218.1 (CO, dd, $^2J_{PC}$ = 22.6 Hz, $^2J_{PC'}$ = 11.3 Hz), 217.7 (CO, d, $^2J_{PC}$ = 10.0 Hz), 141.9–125.2 (phenyl region), 110.1 ($C_\beta$, d, $^3J_{PC}$ = 7.5 Hz), 107.6 ($C_\alpha$, $^2J_{PC}$ = 53.9 Hz, $^2J_{PC'}$ = 11.1 Hz), 31.2 ($CH_2$, t, $^1J_{PC}$ = 25.0 Hz), 22.6 ($CCH_3$, s), 21.3 ($CH_3$, s). $^1H$ NMR ($CDCl_3$, 250 MHz, $\delta$): 7.09–7.75 (phenyl region), 3.29 (dd, $^2J_{PH}$ = 21.9 Hz, $^2J_{HH}$ = 11 Hz), 2.90 ($CH_{2'}$, dd, $^2J_{PH}$ = 21.9 Hz, $^2J_{HH}$ = 11.1 Hz), 0.318 ($CH_3$, s).

**Preparation of $Fe_2(CO)_4(\mu\text{-}PPh_2)(\mu_2\text{-}\eta^2\text{-}C{\equiv}CPh)(\mu\text{-dppe})$ (5A), $Fe_2(CO)_4(\mu\text{-}PPh_2)(\mu_2\text{-}\eta^2\text{-}C{\equiv}CPr^i)(\mu\text{-dppe})$ (5B), and $Fe_2(CO)_4(\mu\text{-}PPh_2)(\mu_2\text{-}\eta^2\text{-}C{\equiv}CBu^t)(\mu\text{-dppe})$ (5C).** A toluene solution of $Fe_2(CO)_6(\mu\text{-}PPh_2)(\mu_2\text{-}\eta^2\text{-}C{\equiv}CPh)$ (0.100 g, 0.176 mmol) was stirred with an equimolar amount of dppe (0.0696 g, 0.176 mmol) for 10 min. The temperature was then raised to 50 °C for a further 1 h. The solution was cooled to room temperature, concentrated to 5 mL, and stored at −10 °C for 48 h. The isolated yield of red-orange crystals was typically 80–90%. $Fe_2(CO)_4(\mu_2\text{-}PPh_2)(\mu_2\text{-}\eta^2\text{-}C{\equiv}CPr^i)(\mu\text{-dppe})$ (**5B**) and $Fe_2(CO)_4(\mu_2\text{-}PPh_2)(\mu_2\text{-}\eta^2\text{-}C{\equiv}CBu^t)(\mu\text{-dppe})$ (**5C**) were prepared in a similar fashion from **1B** and **1C**, respectively.

Anal. Calcd for $C_{50}H_{39}Fe_2O_4P_3$ (**5A**): C, 66.08; H, 4.33. Found: C, 65.89; H, 4.40. IR ($C_6H_{12}$, $\nu$(CO), $cm^{-1}$): 2000 (s), 1949 (vs), 1938 (s), 1904 (m). $^{31}P\{^1H\}$ NMR ($CD_2Cl_2$, 300 K, 101.3 MHz, $\delta$): 147.3 ($\mu$-$PPh_2$, t, $^2J_{PP}$ = 115.3 Hz), 54.0 ($\mu$-dppe, d, $^2J_{PP}$ = 115.3 Hz). $^{13}C\{^1H\}$ NMR ($CD_2Cl_2$, 80.13 MHz, $\delta$): 218.7 (CO, t, $^2J_{PC}$ = 10.0 Hz), 217.4 (CO, dd, $^2J_{PC}$ = 10.0 Hz, $^2J_{PC'}$ = 13.8 Hz), 141.6–127.3 (phenyl region), 103.7 ($C_\alpha$, d, $^2J_{PC}$ = 48.9 Hz), 101.8 ($C_\beta$, d, $^3J_{PC}$ = 15.1 Hz), 21.0 ($CH_2$, d, $^1J_{PC}$ = 22.9 Hz). $^1H$ NMR ($CDCl_3$, 250 MHz, $\delta$): 7.61–6.31 (phenyl region), 2.32 ($CH_2$, dd, $^2J_{PH}$ = 20.6 Hz, $^2J_{HH}$ = 10.0 Hz), 2.08 ($CH_{2'}$, dd, $^2J_{PH}$ = 23 Hz, $^2J_{HH}$ = 10.0 Hz).

Anal. Calcd for $C_{49}H_{41}Fe_2O_4P_3$ (**5B**): C, 65.48; H, 4.60. Found: C, 64.36; H, 4.89. IR ($C_6H_{12}$, $\nu$(CO), $cm^{-1}$): 1998 (s), 1946 (vs), 1932 (s), 1902 (m). $^{31}P\{^1H\}$ NMR ($CD_2Cl_2$, 101.3 MHz, $\delta$): 144.3 ($\mu$-$PPh_2$, t, $^2J_{PP}$ = 118.9 Hz), 50.5 ($\mu$-dppe, d, $^2J_{PP}$ = 118.9 Hz). $^{13}C\{^1H\}$ NMR ($CDCl_3$, 62.8 MHz, $\delta$): 218.6 (CO, dd, $^2J_{PC}$ = $^2J_{PC'}$ = 10.3 Hz), 217.2 (CO, dd, $^2J_{PC}$ = $^2J_{PC'}$ = 23.7 Hz), 141.8–127.0 (phenyl region), 114.2 ($C_\alpha$, dd, $^2J_{PC}$ = 66.8 Hz, $^2J_{PC'}$ = 17.6 Hz), 107.0 ($C_\beta$, d, $^3J_{PC}$ = 8.7 Hz), 25.2 ($CH(CH_3)$–$Pr^i$, s), 22.4 ($CH(CH_3)$–$Pr^i$, s), 21.15 ($CH_2$, d, $^1J_{PC}$ = 22.5 Hz). $^1H$ NMR ($CDCl_3$, 250 MHz, d): 7.78–7.08 (phenyl region), 2.31 ($CH_2$, dd, $^2J_{PH}$ = 20.3 Hz, $^2J_{HH}$ = 9.9 Hz), 2.11 ($CH_{2'}$, dd, $^2J_{PH}$ = 20.0 Hz, $^2J_{HH}$ = 9.9 Hz), 0.51 (CH, sept, $^3J_{HH}$ = 6.4 Hz), 0.13 ($CH_3$, d, $^3J_{HH}$ = 6.4 Hz).

Anal. Calcd for $C_{48}H_{43}Fe_2O_4P_3$ (**5C**): C, 64.86; H, 4.87. Found: C, 64.76; H, 5.05. IR ($C_6H_{12}$, $\nu$(CO), $cm^{-1}$): 2000 (s), 1961 (vs), 1950 (s), 1917 (m). $^{31}P\{^1H\}$ NMR ($CD_2Cl_2$, 80.13 MHz, $\delta$) 144.3 ($\mu$-$PPh_2$, t, $^2J_{PP}$ = 118.3 Hz), 48.9 ($\mu$-dppe, d, $^2J_{PP}$ = 118.8 Hz). $^{13}C\{^1H\}$ NMR ($CDCl_3$, 50.3 MHz, d): 218.77 (CO, dd, $^2J_{PC}$ = 12.2 Hz, $^2J_{PC'}$ = 8.9 Hz), 217.3 (CO, d, $J_{PC}$ = 23.7 Hz), 142.0–127.3 (phenyl region), 114.3 ($C_\beta$, d, $^3J_{PC}$ = 8.4 Hz), 112.6 ($C_\alpha$, dd, $^2J_{PC}$ = 51.9 Hz, $^2J_{PC'}$ = 19.9 Hz), 31.6 ($C(CH_3)_3$, s), 31.5 ($C(CH_3)_3$, s), 21.7 (d, $CH_2$, $^1J_{PC}$ = 21.2 Hz). $^1H$ NMR ($CDCl_3$, 250 MHz, $\delta$): 8.01–7.16 (phenyl region), 2.42 ($CH_2$, ddd, $^2J_{PH}$ = 23.5 Hz, $^3J_{PH}$ = 9.3 Hz, $^2J_{HH}$ = 10.0 Hz), 2.13 ($CH_{2'}$, ddd, $^2J_{PH}$ = 20.2 Hz, $^3J_{HH}$ = 9.3 Hz, $^2J_{HH}$ = 10.0 Hz), 0.26 ($CH_3$, s).

**X-ray Structure Analyses of 2A and 5B.** Yellow-orange crystals of **2A** were grown from a methylene chloride/toluene solution at −10 °C. Red crystals of **5B** were obtained from concentrated toluene solutions at −10 °C. A suitable prism was glued to a glass fiber with epoxy cement, mounted on a goniometer head, and centered on a Syntex $P2_1$ diffractometer. The Syntex autoindexing and cell refinement procedure identified triclinic cells from a set of 25 reflections for **2A** and 27 reflections for **5B**, well dispersed in reciprocal space. Subsequent checks of axial reflections confirmed the lack of systematic absences expected for the triclinic system.

**Collection and Reduction of X-ray Data.** Details of intensity data collection for both compounds are presented in Table I. Both sets of data were collected at 294 K on a Syntex $P2_1$ diffractometer using graphite-monochromated Mo K$\alpha$ ($\lambda$ = 0.71703 Å) radiation and $\theta$–$2\theta$ scans for **2A** and $\omega$ scans for **5B** with a variable scan rate set to optimize measurements of weak reflections. Background measurements using the stationary crystal–stationary counter method were made at the beginning and end of each scan. Two standard reflections monitored after every 100 intensity measurements showed no significant changes (<4%). These were used to scale the data to a common level. Measured reflections were flagged as unobserved when $I < 3\sigma(I)$, where $\sigma$ was derived from counting statistics. Lorentz and polarization corrections were applied to both data sets.

**Solution and Refinement of Intensity Data.** Patterson syntheses readily yielded positions for the two metal atoms in both the compounds. Standard Fourier methods were used to locate the remaining atoms in the molecule, including the disordered solvent molecules (toluene and methylene chloride in **2A**, three molecules of toluene in **5B**). Full-matrix least squares refinements of positional and isotropic thermal parameters and subsequent conversion to anisotropic coefficients for all nonhydrogen atoms and several further cycles of refinement gave $R$ = 0.040 and 0.054 for **2A** and **5B**, respectively. At this stage a difference Fourier map revealed the positions of all the hydrogen atoms. In subsequent refinements to convergence, hydrogen atom positions and isotropic temperature coefficients were included. The function minimized in least-squares calculations was $\sum w = (|F_o| - |F_c|)^2$. The weighted $R$ value is defined as $R_w = [\sum w(|F_o| - |F_c|)^2/\sum w|F_o|^2]^{1/2}$, where the weights, $w$, optimize on moderate intensities. Scattering factors were taken from ref 10, and corrections for anomalous dispersion by the metal atoms were applied. Scattering factors for hydrogen atoms were taken from the data of Stewart et al.[11] The final $R$ and $R_w$ values together with residual electron density levels are given in Table I.

All calculations were carried out on an IBM 4341 network in the University of Waterloo Computing Centre, using a package of programs already described.[4b] Atomic positional parameters for **2A** and **5B** are listed in Tables II and III, respectively; Tables IV and V contain appropriate selections of bond lengths and angles.

## Results and Discussion

**A. Reaction Pathways.** The $^{31}P\{^1H\}$ chemical shifts for the reactants $Fe_2(CO)_6(\mu\text{-}PPh_2)(\mu_2\text{-}\eta^2\text{-}C{\equiv}CR)$, R = Ph ($\delta$ = 148.3 ppm), $Pr^i$ ($\delta$ = 149.7 ppm), $Bu^t$ ($\delta$ = 148.4 ppm),[8]

(10) *International Tables for X-ray Crystallography*; Kynoch Press: Birmingham England, 1974; Vol. IV.
(11) Stewart, R. F.; Davidson, E. R.; Simpson, W. T. *J. Chem. Phys.* **1965**, *42*, 3175.

**Table I. Crystal and Intensity Data for $Fe_2(CO)_5(\mu\text{-}PPh_2)(\mu\text{-}C{=}C(Ph)PPh_2CH_2PPh_2)$ (2A) and $Fe_2(CO)_4(\mu\text{-}PPh_2)(\mu_2\text{-}\eta^2\text{-}C{\equiv}CPr^i)(\mu\text{-dppe})$ (5B)**

| compd | 2A | 5B |
|---|---|---|
| formula | $C_{50}H_{37}Fe_2O_5P\cdot C_7H_8\cdot CH_2Cl_2$ | $C_{47}H_{41}Fe_2O_4P_3\cdot 3C_7H_8$ |
| mol wt | 1099.54 | 1150.889 |
| cryst class | triclinic | triclinic |
| space group | $P\bar{1}$ | $P\bar{1}$ |
| cell constants | | |
| $a$, Å | 10.438 (1) | 10.648 (2) |
| $b$, Å | 12.549 (2) | 12.888 (2) |
| $c$, Å | 21.081 (4) | 23.999 (5) |
| $\alpha$, deg | 85.07 (2) | 77.18 (2) |
| $\beta$, deg | 79.23 (1) | 88.72 (2) |
| $\gamma$, deg | 79.63 (1) | 69.45 (1) |
| $V$, Å$^3$ | 2664.6 (8) | 3001 (1) |
| $Z$ | 2 | 2 |
| $d_{cal}$, (g cm$^{-3}$) | 1.370 | 1.273 |
| $F(000)$ | 1132 | 1204 |
| λ(radiation), Å | 0.710 73 | 0.710 73 |
| temp, K | 294 ± 1 | 294 ± 1 |
| $\mu$(Mo K$\alpha$), cm$^{-1}$ | 7.97 | 6.26 |
| diffractometer | Syntex $P2_1$ | Syntex $P2_1$ |
| cryst size, mm | 0.28 × 0.28 × 0.32 | 0.26 × 0.28 × 0.33 |
| scan type | $\theta$–$2\theta$ | $\omega$ |
| $2\theta$ range, deg | 3.2–45.0 | 3.2–42.0 |
| scan width, deg | 0.8 below K$\alpha_1$ to 0.8 above K$\alpha_2$ | 1.0 |
| scan speed, deg min$^{-1}$ | 3.45–29.30 | 2.02–29.30 |
| std reflns | 533; 008 | 431; 149 |
| variance in stds | ±3% | ±4% |
| transm factors | 0.74 – 0.84 | 0.79 – 0.88 |
| no. of reflns measd | 6999 | 6439 |
| no. of reflns obsd ($I > 3\sigma(I)$) | 5093 | 4195 |
| $R$ | 0.040 | 0.054 |
| $R_w$ | 0.048 | 0.064 |
| weighting scheme, w$^{-1}$ | $2.22 - 0.014\|F_o\| + 0.0006\|F_o\|^2$ | $1.72 - 0.016\|F_o\| + 0.0004\|F_o\|^2$ |
| max residuals, e Å$^{-3}$ | 0.72 ($CH_2Cl_2$) | 0.44 ($C_7H_8$) |

dppm ($\delta$ = −23.6 ppm), and dppe ($\delta$ = −12.4 ppm),[12] are known from previous work. In addition $^{31}P$ data for the isolable intermediate to the bridging diphosphine product, $Fe_2(CO)_5(\mu\text{-}PPh_2)[\mu_2\text{-}C{=}C(Ph)Ph_2PCH_2PPh_2]$ (**2A**) ($\delta$ = 112.6 ppm for the phosphido bridge, $\delta$ = 54.3 ppm for the metal-coordinated dppm phosphorus atom, and $\delta$ = 5.9 ppm for the carbon atom coordinated phosphorus atom), and a structurally characterized product, $Fe_2(CO)_4(\mu_2\text{-}PPh_2)(\mu_2\text{-}\eta^2\text{-}C{\equiv}CPr^i)(\mu\text{-dppe})$ (**5B**) ($\delta$ = 144.3 ppm for $\mu$-$PPh_2$ and $\delta$ = 50.5 for $\mu$ = dppe), were available (Table VI). Thus $^{31}P\{^1H\}$ NMR spectroscopy was an ideal probe to study the reaction pathways. A typical spectral sequence is illustrated in Figure 1. Significant differences in reaction behavior are observed depending upon the nature of the acetylide R group and the diphosphine (Schemes I–III).

Addition of dppm to $Fe_2(CO)_6(\mu\text{-}PPh_2)(\mu_2\text{-}\eta^2\text{-}C{\equiv}CPh)$ at room temperature resulted in the formation of both **2A** and a second complex assigned as $Fe_2(CO)_6(\mu_2\text{-}PPh_2)[\mu\text{-}C{=}C(Ph)Ph_2PCH_2PPh_2]$ (**2A′**). Complex **2A′** exhibited three resonances at 121.8 ($\mu$-$PPh_2$, d, $J$ = 20 Hz), 5.6 [$Ph_2P^+$–C(Ph), dd, $J$ = 64 and 20 Hz], and −27.4 ppm ($Ph_2P$, d, $J$ = 64 Hz) (Table VII), the latter being indicative of uncoordinated phosphorus. In earlier studies[13] it was noted that there exists a clear distinction between $\delta(PPh_2)$ values in complexes having one-carbon three-electron hydrocarbyl ligands (120–160 ppm) and compounds bearing two-carbon three-electron (175–195 ppm) hydrocarbyls. Thus, the chemical shift value of 121.8 ppm for the phosphido bridge in **2** is characteristic of a one-carbon three-electron bridge and can be compared with the value

**Scheme I**

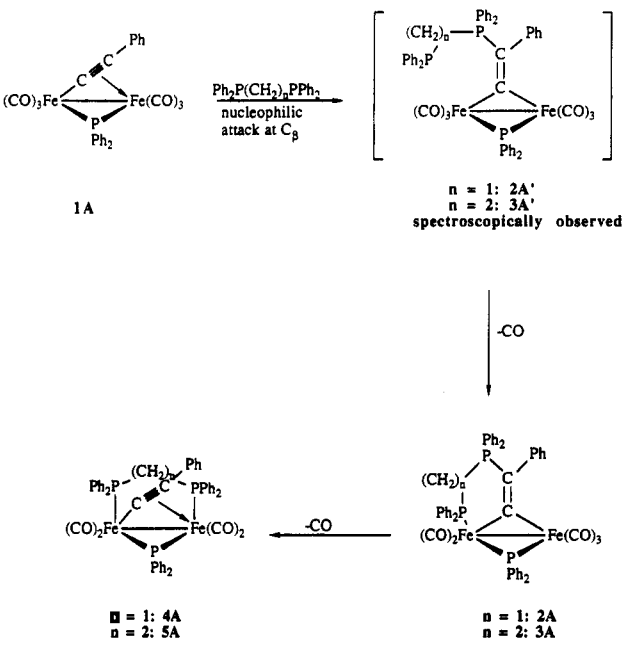


of 122.6 ppm noted for $Fe_2(CO)_6(\mu_2\text{-}PPh_2)[\mu\text{-}C{=}C(Ph)P(Cy)_2H]$, which has been characterized crystallographically.[4k] Upon warming to 50 °C, the resonances due to **2A′** dissappeared with concommitant formation of **2A** as a bright yellow precipitate, confirming that **2A′** is indeed a reaction intermediate (Scheme I).

Reaction of $Fe_2(CO)_6(\mu\text{-}PPh_2)(\mu_2\text{-}\eta^2\text{-}C{\equiv}CPh)$ with dppe follows a similar course (Scheme I). At room temperature an intermediate complex assigned as $Fe_2(CO)_6(\mu\text{-}PPh_2)[\mu\text{-}C{=}C(Ph)PPh_2CH_2CH_2PPh_2]$ (**3A′**) was observed exhibiting resonances at 123.0 ($\mu$-$PPh_2$, d, $J$ = 20 Hz), 6.0

(12) Garrou, P. E. *Chem. Rev.* **1981**, *81*, 229.

(13) MacLaughlin, S. A.; Nucciarone, D.; Carty, A. J. *Phosphorus-31 NMR Spectroscopy in Stereochemical Analysis*; Verkade, J. G., Quinn, L. D., Eds.; Organic Compounds and Metal Complexes; VCH Publishers: New York, 1987; Chapter 16.

**Table II. Atomic Coordinates (Fractional ×10⁴) for Complex 2A with Esds in Parentheses**

| atom | x/a | y/b | z/c |
|---|---|---|---|
| Fe(1) | 1366.6 (6) | 942.0 (5) | 3003.9 (3) |
| Fe(2) | 3094.3 (6) | −402.4 (5) | 2307.1 (3) |
| P(1) | 1187.0 (11) | −749.4 (9) | 2884.5 (5) |
| P(2) | −633.4 (11) | 1829.7 (9) | 3019.5 (5) |
| P(3) | 232.3 (11) | 2484.5 (9) | 1586.5 (5) |
| O(1) | 1493 (5) | 646 (4) | 4383 (2) |
| O(2) | 3126 (4) | 2535 (3) | 2874 (2) |
| O(3) | 5257 (3) | 806 (3) | 1793 (2) |
| O(4) | 3239 (4) | −1913 (3) | 1308 (2) |
| O(5) | 4553 (4) | −1697 (4) | 3252 (2) |
| C(1) | 1435 (5) | 736 (4) | 3843 (2) |
| C(2) | 2390 (5) | 1941 (4) | 2926 (2) |
| C(3) | 4411 (4) | 332 (4) | 1991 (2) |
| C(4) | 3199 (4) | −1306 (4) | 1693 (2) |
| C(5) | 3987 (4) | −1200 (4) | 2886 (3) |
| C(6) | −1056 (4) | 2073 (4) | 2203 (2) |
| C(7) | 1867 (4) | 871 (3) | 2074 (2) |
| C(8) | 1643 (4) | 1460 (3) | 1529 (2) |
| C(9) | 2462 (4) | 1299 (3) | 863 (2) |
| C(10) | 3523 (5) | 1837 (4) | 657 (2) |
| C(11) | 4283 (5) | 1701 (5) | 41 (3) |
| C(12) | 3984 (5) | 1043 (5) | −369 (2) |
| C(13) | 2935 (5) | 504 (4) | −176 (2) |
| C(14) | 2171 (5) | 632 (4) | 441 (2) |
| C(15) | 1273 (4) | −1842 (4) | 3512 (2) |
| C(16) | 688 (7) | −1712 (5) | 4149 (3) |
| C(17) | 860 (8) | −2587 (6) | 4615 (3) |
| C(18) | 1566 (8) | −3554 (5) | 4432 (3) |
| C(19) | 2112 (6) | −3694 (5) | 3802 (3) |
| C(20) | 1967 (5) | −2854 (4) | 3348 (3) |
| C(21) | −107 (4) | −1069 (3) | 2491 (2) |
| C(22) | −1178 (5) | −1462 (4) | 2858 (3) |
| C(23) | −2205 (5) | −1646 (5) | 2562 (3) |
| C(24) | −2173 (6) | −1438 (4) | 1917 (4) |
| C(25) | −1102 (6) | −1062 (5) | 1546 (3) |
| C(26) | −77 (5) | −874 (4) | 1834 (2) |
| C(27) | −2038 (4) | 1202 (3) | 3428 (2) |
| C(28) | −2036 (5) | 788 (5) | 4052 (2) |
| C(29) | −3062 (6) | 292 (6) | 4395 (3) |
| C(30) | −4125 (5) | 232 (6) | 4116 (3) |
| C(31) | −4167 (5) | 645 (5) | 3499 (2) |
| C(32) | −3137 (4) | 1121 (4) | 3156 (2) |
| C(33) | −1104 (5) | 3186 (4) | 3344 (2) |
| C(34) | −207 (6) | 3667 (5) | 3559 (3) |
| C(35) | −561 (9) | 4706 (6) | 3796 (4) |
| C(36) | −1807 (9) | 5242 (5) | 3820 (3) |
| C(37) | −2715 (9) | 4775 (6) | 3611 (4) |
| C(38) | −2380 (7) | 3759 (5) | 3372 (3) |
| C(39) | 445 (4) | 3820 (3) | 1753 (2) |
| C(40) | 1657 (5) | 4060 (4) | 1789 (2) |
| C(41) | 1773 (7) | 5112 (4) | 1917 (3) |
| C(42) | 662 (7) | 5879 (4) | 2023 (3) |
| C(43) | −549 (6) | 5646 (4) | 1987 (3) |
| C(44) | −673 (5) | 4625 (4) | 1851 (2) |
| C(45) | −372 (4) | 2642 (3) | 830 (2) |
| C(46) | 130 (6) | 3354 (5) | 351 (2) |
| C(47) | −245 (7) | 3441 (5) | −252 (3) |
| C(48) | −1145 (7) | 2830 (5) | −370 (3) |
| C(49) | −1640 (7) | 2132 (5) | 102 (3) |
| C(50) | −1266 (6) | 2037 (4) | 701 (2) |

**Table III. Atomic Coordinates (Fractional ×10⁴) for Complex 5B with Esds in Parentheses**

| atom | x/a | y/b | z/c | U(eq), Å² |
|---|---|---|---|---|
| Fe(1) | 1453.3 (11) | 3700.0 (8) | 3162.8 (4) | 50 |
| Fe(2) | 288.0 (10) | 5630.2 (8) | 2419.3 (4) | 46 |
| P(1) | 896 (2) | 5408 (2) | 3330.4 (8) | 47 |
| P(2) | 1651 (2) | 2363 (2) | 2692.3 (8) | 48 |
| P(3) | −136 (2) | 5164 (2) | 1609.1 (8) | 46 |
| O(1) | 1697 (7) | 2302 (5) | 4312 (2) | 87 |
| O(2) | 4303 (6) | 3343 (5) | 3080 (3) | 88 |
| O(3) | −1095 (6) | 8088 (5) | 2131 (3) | 84 |
| O(4) | 2946 (6) | 5615 (5) | 2103 (2) | 79 |
| C(1) | 1605 (9) | 2837 (7) | 3854 (3) | 69 |
| C(2) | 3158 (8) | 3491 (6) | 3122 (3) | 60 |
| C(3) | −607 (8) | 7115 (7) | 2233 (3) | 64 |
| C(4) | 1897 (8) | 5601 (6) | 2228 (3) | 55 |
| C(5) | −386 (7) | 4371 (6) | 2926 (3) | 50 |
| C(6) | −1518 (8) | 5117 (6) | 2748 (3) | 56 |
| C(7) | −2998 (7) | 5691 (7) | 2677 (4) | 66 |
| C(8) | −3647 (9) | 4872 (9) | 2993 (5) | 108 |
| C(9) | −3450 (9) | 6814 (8) | 2858 (5) | 98 |
| C(10) | 2171 (7) | 5934 (6) | 3532 (3) | 56 |
| C(11) | 3060 (8) | 5294 (7) | 4001 (3) | 67 |
| C(12) | 3966 (9) | 5727 (9) | 4185 (4) | 83 |
| C(13) | 3965 (9) | 6811 (8) | 3920 (4) | 87 |
| C(14) | 3075 (9) | 7434 (7) | 3445 (4) | 82 |
| C(15) | 2179 (8) | 7003 (7) | 3249 (3) | 70 |
| C(16) | −384 (7) | 5886 (6) | 3835 (3) | 53 |
| C(17) | −937 (9) | 5127 (7) | 4162 (3) | 60 |
| C(18) | −1930 (10) | 5528 (8) | 4544 (4) | 92 |
| C(19) | −2351 (9) | 6649 (8) | 4601 (4) | 79 |
| C(20) | −1779 (9) | 7392 (8) | 4275 (4) | 82 |
| C(21) | −786 (8) | 7017 (6) | 3889 (3) | 65 |
| C(22) | 1484 (7) | 2824 (6) | 1901 (3) | 54 |
| C(23) | 21 (7) | 3655 (6) | 1701 (3) | 55 |
| C(24) | 508 (7) | 1563 (6) | 2852 (3) | 53 |
| C(25) | −454 (8) | 1810 (7) | 3251 (4) | 73 |
| C(26) | −1295 (10) | 1144 (8) | 3392 (4) | 97 |
| C(27) | −1135 (10) | 263 (8) | 3106 (5) | 94 |
| C(28) | −172 (10) | 40 (7) | 2703 (5) | 86 |
| C(29) | 660 (8) | 681 (6) | 2564 (4) | 69 |
| C(30) | 3280 (8) | 1192 (6) | 2827 (3) | 58 |
| C(31) | 3483 (8) | 435 (7) | 3374 (4) | 70 |
| C(32) | 4765 (10) | −441 (7) | 3523 (4) | 84 |
| C(33) | 5748 (9) | −549 (7) | 3128 (5) | 82 |
| C(34) | 5538 (9) | 189 (9) | 2592 (5) | 91 |
| C(35) | 4260 (9) | 1072 (7) | 2437 (4) | 78 |
| C(36) | 852 (7) | 5428 (6) | 989 (3) | 53 |
| C(37) | 1233 (8) | 6390 (7) | 907 (3) | 69 |
| C(38) | 1953 (10) | 6648 (9) | 423 (4) | 88 |
| C(39) | 2297 (9) | 5911 (10) | 37 (4) | 83 |
| C(40) | 1920 (9) | 4945 (9) | 125 (4) | 85 |
| C(41) | 1185 (8) | 4705 (7) | 603 (3) | 64 |
| C(42) | −1852 (7) | 5915 (6) | 1284 (3) | 52 |
| C(43) | −2238 (9) | 7103 (7) | 1055 (3) | 69 |
| C(44) | −3554 (9) | 7719 (8) | 810 (4) | 82 |
| C(45) | −4487 (10) | 7185 (9) | 815 (4) | 90 |
| C(46) | −4116 (8) | 6007 (8) | 1039 (4) | 79 |
| C(47) | −2763 (7) | 5368 (7) | 1272 (3) | 66 |

[$PhP^+$–C(Ph), dd, $J_{PP}$ = 39 Hz, $J_{PP}$ = 20 Hz], and −11.8 ppm ($Ph_2P$, d, $J_{PP}$ = 39 Hz). Upon warming to 60 °C, **3A′** was converted cleanly into **5A**. Although no reaction intermediates were observed, by analogy to the reaction with dppm, a further intermediate (**3A**) in which the dppm ligand forms part of an unstable seven-membered ring is postulated which rapidly converts via carbonyl loss to the observed reaction product **5A**.

Although the dppm analogue of **5A** could not be prepared via the direct addition of the ligand to $Fe_2(CO)_6(\mu\text{-}PPh_2)(\mu_2\text{-}\eta^2\text{-}C{\equiv}CPh)$ due to the preferential nucleophilic attack at the β-carbon of the σ–π acetylide ligand, an alternative synthetic scheme was devised utilizing the precoordination of the diphosphine to the dimetal center (eq 1). UV irradiation of a THF solution of $Fe_2(CO)_6(\mu\text{-}CO)(\mu\text{-dppm})$[9,14] and $Ph_2PC{\equiv}CPh$ resulted in the isolation of $Fe_2(CO)_4(\mu_2\text{-}PPh_2)(\mu_2\text{-}\eta^2\text{-}C{\equiv}CPh)(\mu\text{-dppm})$ (**4A**) in 85–90% yield via the facile cleavage of the P–C(sp) bond of the phosphinoalkyne. The structure of **4A** was readily

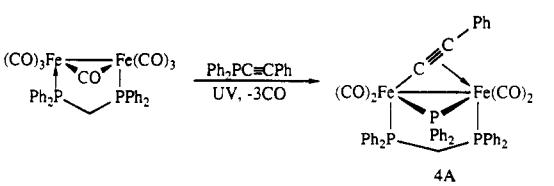


4A (1)

(14) Hogarth, G.; Kayser, F.; Knox, S. A. R.; Morton, D. A. V.; Orpen, A. G.; Turner, M. L. *J. Chem. Soc., Chem. Commun.* **1988**, 358.

**Table IV. Selected Interatomic Distances (Å) and Bond Angles (deg) for 2A with Esds in Parentheses**

| | | | |
|---|---|---|---|
| Fe(1)–Fe(2) | 2.5683 (8) | Fe(1)–P(1) | 2.204 (1) |
| Fe(1)–P(2) | 2.178 (1) | Fe(2)–P(1) | 2.225 (1) |
| Fe(1)–C(1) | 1.780 (5) | Fe(1)–C(2) | 1.766 (5) |
| Fe(1)–C(7) | 1.938 (4) | Fe(2)–C(3) | 1.786 (5) |
| Fe(2)–C(4) | 1.769 (5) | Fe(2)–C(5) | 1.799 (5) |
| Fe(2)–C(7) | 1.949 (4) | P(1)–C(15) | 1.824 (4) |
| P(1)–C(21) | 1.829 (4) | P(2)–C(6) | 1.823 (4) |
| P(2)–C(27) | 1.827 (4) | P(2)–C(33) | 1.838 (4) |
| P(3)–C(6) | 1.802 (4) | P(3)–C(8) | 1.765 (4) |
| P(3)–C(39) | 1.802 (4) | P(3)–C(45) | 1.804 (4) |
| C(1)–O(1) | 1.144 (6) | C(2)–O(2) | 1.150 (6) |
| C(3)–O(3) | 1.149 (6) | C(4)–O(4) | 1.151 (6) |
| C(5)–O(5) | 1.136 (7) | C(7)–C(8) | 1.346 (5) |
| C(8)–C(9) | 1.511 (6) | | |
| Fe(2)–Fe(1)–P(1) | 54.94 (3) | Fe(2)–Fe(1)–P(2) | 139.59 (3) |
| Fe(2)–Fe(1)–C(1) | 113.0 (2) | Fe(2)–Fe(1)–C(2) | 94.4 (1) |
| Fe(2)–Fe(1)–C(7) | 48.8 (1) | P(1)–Fe(1)–P(2) | 103.93 (4) |
| P(1)–Fe(1)–C(1) | 94.6 (2) | P(1)–Fe(1)–C(2) | 148.3 (2) |
| P(1)–Fe(1)–C(7) | 79.3 (1) | P(2)–Fe(1)–C(1) | 101.7 (2) |
| P(2)–Fe(1)–C(2) | 105.6 (2) | P(2)–Fe(1)–C(7) | 97.3 (1) |
| C(1)–Fe(1)–C(2) | 90.5 (2) | C(1)–Fe(1)–C(7) | 160.9 (2) |
| C(2)–Fe(1)–C(7) | 85.8 (2) | Fe(1)–Fe(2)–P(1) | 54.17 (3) |
| Fe(1)–Fe(2)–C(3) | 104.7 (1) | Fe(1)–Fe(2)–C(4) | 139.9 (1) |
| Fe(1)–Fe(2)–C(5) | 103.4 (2) | Fe(1)–Fe(2)–C(7) | 48.5 (1) |
| P(1)–Fe(2)–C(3) | 158.8 (1) | P(1)–Fe(2)–C(4) | 96.8 (1) |
| P(1)–Fe(2)–C(5) | 90.6 (2) | P(1)–Fe(2)–C(7) | 78.6 (1) |
| C(3)–Fe(2)–C(4) | 102.4 (2) | C(3)–Fe(2)–C(5) | 93.5 (2) |
| C(3)–Fe(2)–C(7) | 88.0 (2) | C(4)–Fe(2)–C(5) | 103.8 (2) |
| C(4)–Fe(2)–C(7) | 104.3 (2) | C(5)–Fe(2)–C(7) | 150.8 (2) |
| Fe(1)–P(1)–Fe(2) | 70.89 (3) | Fe(1)–P(1)–C(15) | 125.1 (1) |

**Table V. Selected Interatomic Distances (Å) and Bond Angles (deg) for 5B with Esds in Parentheses**

| | | | |
|---|---|---|---|
| Fe(1)–Fe(2) | 2.622 (1) | Fe(1)–P(1) | 2.197 (2) |
| Fe(1)–P(2) | 2.211 (2) | Fe(1)–C(1) | 1.755 (8) |
| Fe(1)–C(2) | 1.742 (9) | Fe(1)–C(5) | 1.883 (8) |
| Fe(2)–P(1) | 2.222 (2) | Fe(2)–P(3) | 2.257 (2) |
| Fe(2)–C(3) | 1.769 (8) | Fe(2)–C(4) | 1.754 (9) |
| Fe(2)–C(5) | 2.128 (7) | Fe(2)–C(6) | 2.314 (8) |
| P(1)–C(10) | 1.832 (8) | P(1)–C(16) | 1.835 (8) |
| P(2)–C(22) | 1.852 (7) | P(2)–C(24) | 1.837 (8) |
| P(2)–C(30) | 1.833 (8) | P(3)–C(23) | 1.855 (7) |
| P(3)–C(36) | 1.841 (7) | P(3)–C(42) | 1.837 (8) |
| C(1)–O(1) | 1.147 (10) | C(2)–O(2) | 1.172 (11) |
| C(3)–O(3) | 1.146 (10) | C(4)–O(4) | 1.155 (11) |
| C(5)–C(6) | 1.261 (11) | C(6)–C(7) | 1.482 (12) |
| C(7)–C(8) | 1.517 (14) | C(7)–C(9) | 1.516 (14) |
| C(22)–C(23) | 1.562 (11) | | |
| Fe(2)–Fe(1)–P(1) | 54.05 (5) | Fe(2)–Fe(1)–P(2) | 105.17 (5) |
| Fe(2)–Fe(1)–C(1) | 150.3 (3) | Fe(2)–Fe(1)–C(2) | 103.5 (3) |
| Fe(2)–Fe(1)–C(5) | 53.4 (2) | P(1)–Fe(1)–P(2) | 159.19 (7) |
| P(1)–Fe(1)–C(1) | 102.5 (3) | P(1)–Fe(1)–C(2) | 94.6 (3) |
| P(1)–Fe(1)–C(5) | 77.0 (2) | P(2)–Fe(1)–C(1) | 96.7 (3) |
| P(2)–Fe(1)–C(2) | 91.5 (3) | P(2)–Fe(1)–C(5) | 89.5 (2) |
| C(1)–Fe(1)–C(2) | 95.7 (4) | C(1)–Fe(1)–C(5) | 108.0 (4) |
| C(2)–Fe(1)–C(5) | 156.0 (3) | Fe(1)–Fe(2)–P(1) | 53.16 (5) |
| Fe(1)–Fe(2)–P(3) | 106.08 (5) | Fe(1)–Fe(2)–C(3) | 152.7 (3) |
| Fe(1)–Fe(2)–C(4) | 87.8 (3) | Fe(1)–Fe(2)–C(5) | 45.3 (2) |
| Fe(1)–Fe(2)–C(6) | 77.6 (2) | P(1)–Fe(2)–P(3) | 158.98 (7) |
| P(1)–Fe(2)–C(3) | 100.4 (3) | P(1)–Fe(2)–C(4) | 89.7 (3) |
| P(1)–Fe(2)–C(5) | 71.8 (2) | P(1)–Fe(2)–C(6) | 87.2 (2) |
| P(3)–Fe(2)–C(3) | 99.7 (3) | P(3)–Fe(2)–C(4) | 92.9 (3) |
| P(3)–Fe(2)–C(5) | 91.2 (2) | P(3)–Fe(2)–C(6) | 84.5 (2) |
| C(3)–Fe(2)–C(4) | 99.9 (4) | C(3)–Fe(2)–C(5) | 126.6 (3) |
| C(3)–Fe(2)–C(6) | 96.4 (3) | C(4)–Fe(2)–C(5) | 131.7 (3) |
| C(4)–Fe(2)–C(6) | 163.7 (3) | C(5)–Fe(2)–C(6) | 32.6 (3) |
| Fe(1)–P(1)–Fe(2) | 72.79 (5) | Fe(1)–P(1)–C(10) | 121.3 (2) |

established by IR and $^{31}P$ NMR spectroscopy.

The complex $Fe_2(CO)_6(\mu\text{-}CO)(\mu\text{-}dppm)$ has previously been shown to activate "internal" phosphorus–methylene bonds of the dppm ligand.[6] The above reaction represents the activation of an "external" phosphorus–carbon bond by the same complex and is perhaps a general phenomenon. (The phosphinoalkyne is almost certainly pre-

**Table VI. $^{31}P\{^1H\}$ NMR Data for the Reaction Products $Fe_2(CO)_4(\mu\text{-}PPh_2)(\mu_2\text{-}\eta^2\text{-}C_2R)(\mu\text{-dppm})$ and $Fe_2(CO)_4(\mu\text{-}PPh_2)(\mu_2\text{-}\eta^2\text{-}C_2R)(\mu\text{-dppe})$**

| complex | ligand | chemical shift, ppm | multiplicity | coupling constant, Hz |
|---|---|---|---|---|
| **2A** | $\mu$-$PPh_2$ | 112.6 | d | $^4J_{PP}$ = 13.5 |
| | Fe-$PPh_2$ | 54.3 | d | $^2J_{PP}$ = 18.1 |
| | C-$PPh_2$ | 5.9 | dd | 18.1/13.8 |
| **5A** | $\mu$-$PPh_2$ | 147.3 | t | $^2J_{PP}$ = 115.3 |
| | $\mu$-dppe | 54.0 | d | $^2J_{PP}$ = 115.3 |
| **4B** | $\mu$-$PPh_2$ | 179.8 | t | $^2J_{PP}$ = 119.1 |
| | $\mu$-dppm | 60.5 | d | $^2J_{PP}$ = 119.1 |
| **5B** | $\mu$-$PPh_2$ | 144.3 | t | $^2J_{PP}$ = 119.0 |
| | $\mu$-dppe | 50.5 | d | $^2J_{PP}$ = 119.0 |
| **4C** | $\mu$-$PPh_2$ | 180.9 | t | $^2J_{PP}$ = 122.5 |
| | $\mu$-dppm | 54.3 | d | $^2J_{PP}$ = 112.5 |
| **5C** | $\mu$-$PPh_2$ | 144.9 | t | $^2J_{PP}$ = 117.0 |
| | $\mu$-dppe | 49.7 | d | $^2J_{PP}$ = 117.0 |
| **4A** | $\mu$-$PPh_2$ | 178.3 | t | $^2J_{PP}$ = 114.5 |
| | $\mu$-dppm | 58.5 | d | $^2J_{PP}$ = 114.5 |

**Table VII. $^{31}P\{^1H\}$ NMR Data for the dppm and dppe Intermediates**

| complex | ligand | chemical shift, ppm | multiplicity | coupling constant, Hz |
|---|---|---|---|---|
| **2A′** | $\mu$-$PPh_2$ | 121.8 | d | $^4J_{PP}$ = 19.4 |
| | coordinated | | | $^2J_{PP}$ = 63.9 |
| | C-$P$$Ph_2CH_2PPh_2$ | 5.5 | dd | $^4J_{PP}$ = 19.3 |
| | uncoordinated | | | |
| | C-$PPh_2CH_2$$P$$Ph_2$ | −27.4 | d | $^2J_{PP}$ = 63.9 |
| **3A′** | $\mu$-$PPh_2$ | 122.6 | d | $^4J_{PP}$ = 17.8 |
| | coordinated | | | $^3J_{PP}$ = 40.8 |
| | C-$P$$Ph_2(CH_2)_2PPh_2$ | 6.8 | dd | $^4J_{PP}$ = 17.8 |
| | uncoordinated | | | |
| | C-$PPh_2(CH_2)_2$$P$$Ph_2$ | −12.0 | d | $^3J_{PP}$ = 40.8 |
| **2B″** | $\mu$-$PPh_2$ | 152.4 | broad | |
| | coordinated | | | |
| | $\mu$-$P$$Ph_2CH_2PPh_2$ | 50.2 | broad | |
| | uncoordinated | | | |
| | $\mu$-$PPh_2CH_2$$P$$Ph_2$ | −21.2 | broad | |
| **3B″** | $\mu$-$PPh_2$ | 151.8 | d | $^2J_{PP}$ = 96.0 |
| | coordinated | | | $^2J_{PP}$ = 96.0 |
| | $\mu$-$P$$Ph_2(CH_2)_2PPh_2$ | 55.3 | dd | $^3J_{PP}$ = 37.2 |
| | uncoordinated | | | |
| | $\mu$-$PPh_2(CH_2)_2$$P$$Ph_2$ | −13.0 | d | $^3J_{PP}$ = 37.2 |
| **3B** | $\mu$-$PPh_2$ | 126.5 | d | $^4J_{PP}$ = 55.1 |
| | $\mu$-$P$$Ph_2(CH_2)_2PPh_2$ | 52.3 | dd | $^4J_{PP}$ = 55.1 |
| | $\mu$-$PPh_2(CH_2)_2$$P$$Ph_2$ | 2.3 | d | $^3J_{PP}$ = 2.3 |
| | | | | $^3J_{PP}$ = 2.3 |
| **2C″** | $\mu$-$PPh_2$ | 153.4 | d | $^2J_{PMP}$ = 95.8 |
| | coordinated | | | $^2J_{PMP}$ = 95.8 |
| | $\mu$-$P$$Ph_2CH_2PPh_2$ | 53.9 | dd | $^2J_{PCP}$ = 66.0 |
| | uncoordinated | | | |
| | $\mu$-$PPh_2CH_2$$P$$Ph_2$ | −25.7 | d | $^2J_{PCP}$ = 66.0 |
| **3C″** | $\mu$-$PPh_2$ | 153.3 | d | $^2J_{PMP}$ = 94.7 |
| | coordinated | | | $^2J_{PMP}$ = 94.7 |
| | $\mu$-$P$$Ph_2(CH_2)_2PPh_2$ | 57.1 | dd | $^3J_{PCCP}$ = 37.8 |
| | uncoordinated | | | |
| | $\mu$-$PPh_2(CH_2)_2$$P$$Ph_2$ | −11.8 | d | $^2J_{PCCP}$ = 37.8 |

coordinated to the dimetal center prior to the cleavage reaction, the latter, however, being so facile that no such intermediate complex could be observed.) The facile activation of P–C(sp) bonds has been well established in previous work in this laboratory,[15] and indeed, P–C bond cleavage of phosphinoalkynes is a useful synthetic route to $\mu$-phosphido and $\mu$-alkynyl polynuclear compounds. More recently, the activation of a P–C(sp) bond via UV-

(15) (a) Carty, A. J. *ACS Adv. Chem. Ser.* **1982**, *196*, 163. (b) Carty, A. J. *Pure Appl. Chem.* **1982**, *54*, 113. (c) Van Gastel, F.; MacLaughlin, S. A.; Lynch, M.; Carty, A. J.; Sappa, E.; Tiripicchio, A.; Tiripicchio-Camellini, M. *J. Organomet. Chem.* **1987**, *326*, C65. (d) Garrou, P. E. *Chem. Rev.* **1985**, *85*, 171.

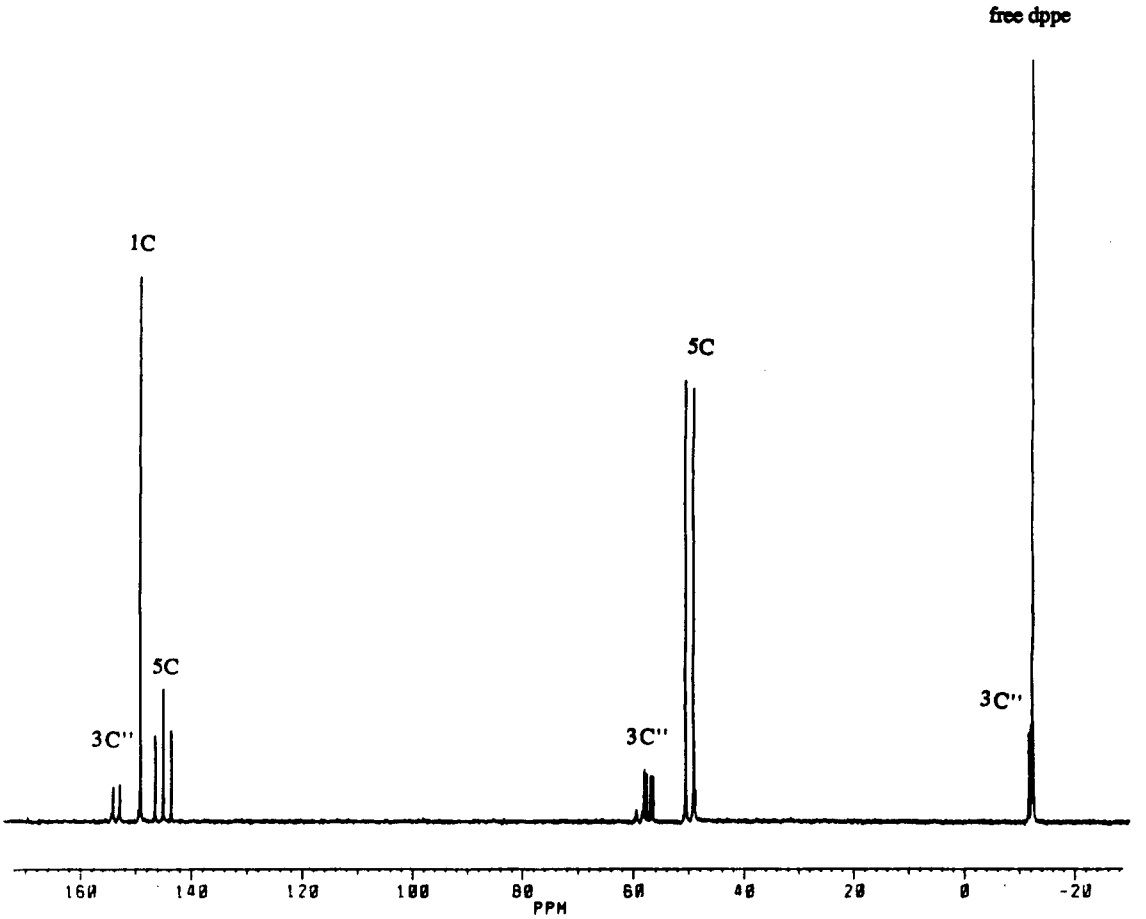


**Figure 1.** $^{31}P\{^1H\}$ spectrum of a reaction mixture of $Fe_2(CO)_6(\mu\text{-}PPh_2)(\mu_2\text{-}\eta^2\text{-}C{\equiv}CBu^t)$ (**1C**) and dppe. Intermediates and products are as follows: **3C''**, $Fe_2(CO)_5(\mu\text{-}PPh_2)(\mu_2\text{-}\eta^2\text{-}C{\equiv}CBu^t)(\eta^1\text{-}Ph_2P(CH_2)_2PPh_2)$; **5C**, $Fe_2(CO)_4(\mu\text{-}PPh_2)(\mu_2\text{-}\eta^2\text{-}C{\equiv}CBu^t)(\mu\text{-dppe})$.

induced coordination to a transition-metal center has been reported.[16] Complex **4A** was also produced during an investigation of the thermal stability of **2A**. Thus, upon prolonged reflux (~2 weeks in THF), slow carbon monoxide evolution was noted, forming a solution from which **4A** was isolated in 70–80% yield as the only reaction product. The reverse of this transformation, namely **4A** to **2A** (eq 2) could not, however, be induced even after

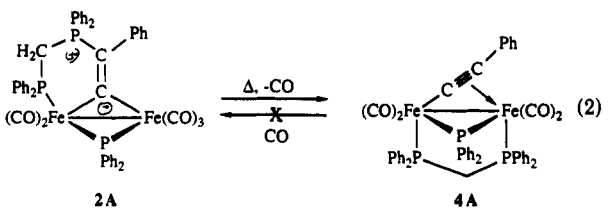


(2)

**2A** **4A**

prolonged exposure of **4A** to carbon monoxide, demonstrating the stability incurred by the strong metal–phosphorus interactions. The formation of **4A** from **2A** provides further evidence that the reaction of dppe with $Fe_2(CO)_6(\mu_2\text{-}PPh_2)(\mu_2\text{-}\eta^2\text{-}C{\equiv}CPh)$ proceeds via an intermediate (**3A**) in which the diphosphine spans metal and carbon sites. The vastly differing rate (2 min vs 2 weeks) of phosphorus–carbon bond cleavage between the dppe and dppm intermediates can be attributed to the relative stability of six- vs seven-membered ring systems.

In the case of isopropylacetylide the carbon-bound intermediate **2B** formed in the reaction with dppm (Scheme II) is very insoluble and precipitates from solution. In an effort to dissolve enough of this compound for $^{31}P\{^1H\}$ characterization, the mixture was heated at 90 °C for 3 h but this led overwhelmingly to the $\mu$-dppm product **4B**. If the dppm is added to $Fe_2(CO)_6(\mu_2\text{-}PPh_2)(\mu_2\text{-}\eta^2\text{-}C{\equiv}CPr^i)$ at 50 °C, a different pathway (pathway I, Scheme II), via a sequential CO substitution (intermediate **2B''**), first on Fe(1) then on Fe(2) appears to result in the formation of **4B** (Tables VI and VII).

The complex $Fe_2(CO)_6(\mu_2\text{-}PPh_2)(\mu_2\text{-}\eta^2\text{-}C{\equiv}CPr^i)$ reacts cleanly with dppe at elevated temperatures to form **5B**. At room temperature however two separate pathways are observed (Scheme II). A set of signals at $\delta$ 126.5, 52.3, and 2.3 ppm correspond to the phosphido bridge, the Fe-bound phosphorus atom, and the dppe C-bound phosphorus atom of the vinylidene intermediate **3B**, respectively. A second intermediate has signals at 151.8, 55.8, and −13.0 ppm corresponding to a phosphido bridge, an M-bound dppe phosphorus atom, and a free dppe phosphorus atom of **3B''**. Although there is no spectroscopic evidence for the C-bound dppe with one free dppe phosphorus atom (intermediate **3B'**), **3B** is thought to be formed via intermediate **3B'** by analogy with the formation of **2A** from **2A'**. There is no evidence for the formation of the insoluble intermediate **3B** during the conversion of **3B''** to **4B**. The two pathways (1 and 2) may be separate, or **3B** may be the precursor of **3B''** (Scheme II).

In reactions of dppm and dppe with the *tert*-butylacetylide $Fe_2(CO)_6(\mu_2\text{-}PPh_2)(\mu_2\text{-}\eta^2\text{-}C{\equiv}CBu^t)$ (**1C**) there is no spectroscopic evidence for nucleophilic attack at either carbon of the acetylide to form adduct **2C** or **3C**. Only the metal-coordinated intermediates **2C''** and **3C''** are observed. The reaction proceeds smoothly to form **4C** and **5C** (Scheme III).

It is clear from the above results that there are differences between dppm and dppe in the mechanisms of at-

(16) Cherkas, A. A. Ph.D. Thesis, University of Waterloo, 1989.

**Scheme II**

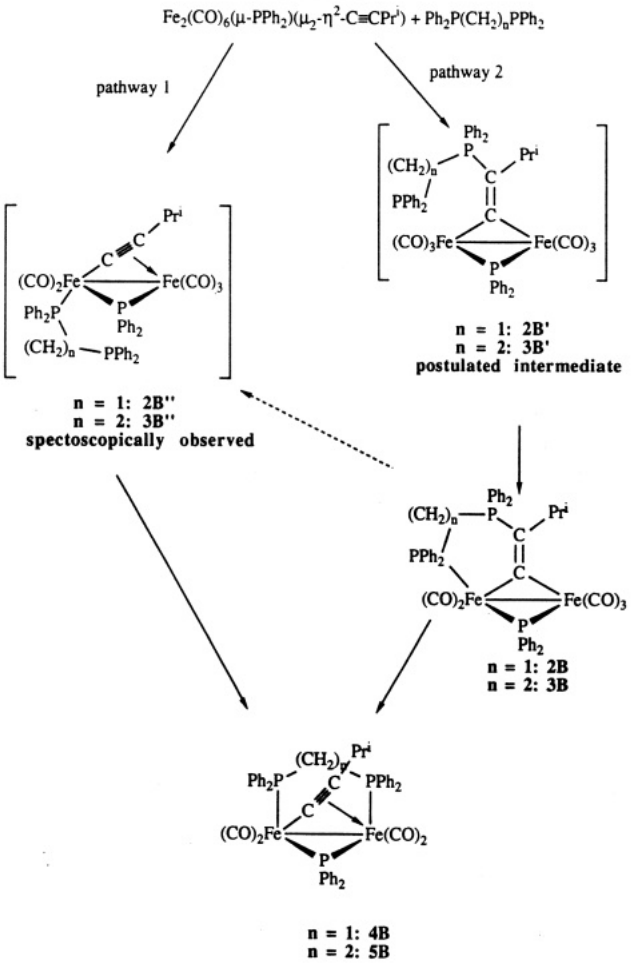


**Scheme III**

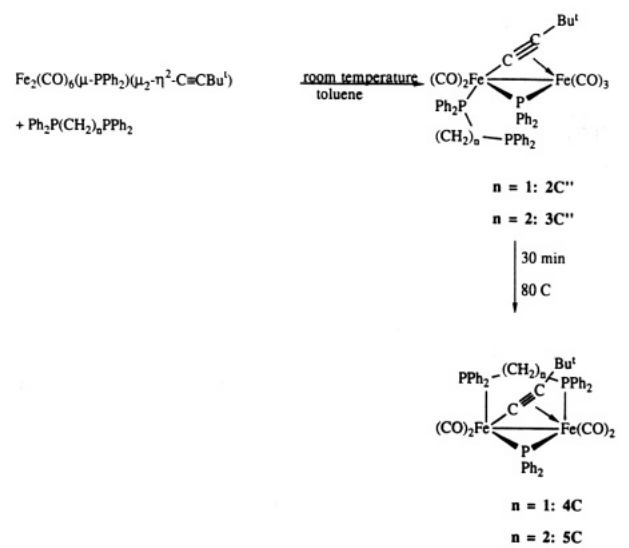


tack on these carbonyl acetylides. The reaction pathway also changes as the R group on the acetylide varies. As the steric bulk of the acetylide R group increases (Ph < $Pr^i$ < $Bu^t$), the reaction pathway moves from initial nucleophilic attack at $C_\beta$ of the acetylide, generating a C-coordinated phosphine, to attack at the metal center. A bulkier R group may prevent the incoming nucleophile from approaching $C_\beta$ for coordination. Extended Huckel molecular orbital calculations on the model compound $Fe_2(CO)_6(\mu\text{-}PH_2)(\mu_2\text{-}\eta^2\text{-}C{\equiv}CH)$ have shown that, in the dynamic $\sigma$–$\pi$ exchange process for the $\mu_2$-$\eta^2$ acetylide (vide

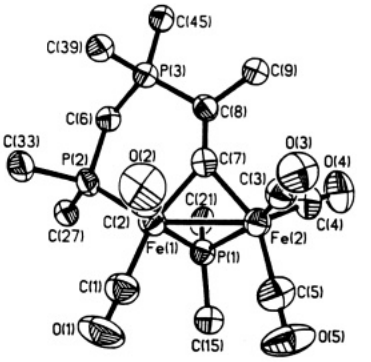


**Figure 2.** Perspective view of the molecular structure of the zwitterionic vinylidene complex $Fe_2(CO)_5(\mu\text{-}PPh_2)(\mu\text{-}C{=}C(Ph)\text{-}Ph_2PCH_2PPh_2)$ (**2A**).

infra), there is a component of the LUMO on $C_\beta$ which can bond to an incoming nucleophile.[16] If this pathway is blocked, the remaining portion of the LUMO is on the metal atoms which would then become the site of nucleophilic attack as in I. A phenyl group, which is smaller

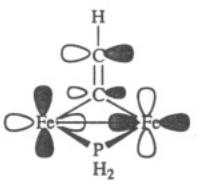

I

LUMO of $Fe_2(CO)_6(\mu\text{-}PH_2)(\mu_2\text{-}\eta^1\text{-}C{\equiv}CH)$

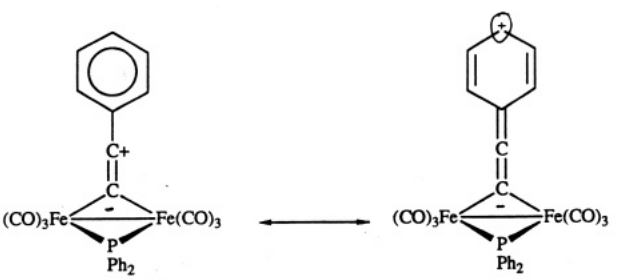

IIa (II) IIb

Possible stabilising resonance structures for the transition state (I)

than a tertiary butyl group, can also stabilize this transition state through resonance (as shown in IIa and IIb), which would also direct the nucleophilic addition to $C_\beta$ for R = Ph over R = $Pr^i$ or $Bu^t$.

As part of the reaction mechanism, the metal-coordinated phosphorus atom of the diphosphine in the vinylidene type structure **2A** must move from a position cis to the phosphido bridge, as evidenced from the lack of a $^2J_{PPh_2\text{-}P_{diphos}}$ coupling constant in **2A** and shown in the crystal structure (Figure 2), to a position trans to the phosphido bridge as in **4A**. The large $^2J_{PPh_2\text{-}P_{diphos}}$ coupling constant of 114.5 Hz in **4A** (Table VI) and the crystal structure of **5B** confirm this stereochemical change. Indeed, large trans $^{31}P$–$^{31}P$ coupling constants facilitate the identification of metal-coordinated intermediates such as **3B''** ($^2J_{PP}$ = 96 Hz).

**B. Spectroscopic Features.** The infrared spectra of the $\mu$-dppm and $\mu$-dppe products **4A–C** and **5A-C** are all similar in the $\nu$(CO) region, showing four terminal carbonyl bands.

In the $^{13}C\{^1H\}$ NMR spectra of **4A–C** and **5A–C** only two resonances for carbonyl carbon atoms are observed, corresponding to the pair of CO groups trans to the metal–

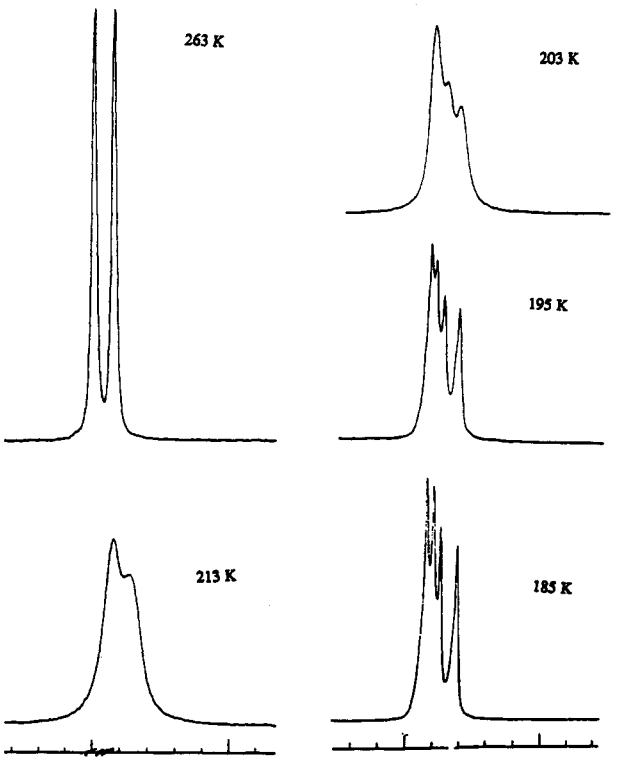


**Figure 3.** Variable-temperature $^{31}P\{^1H\}$ NMR spectra of the complex $Fe_2(CO)_4(\mu\text{-}PPh_2)(\mu_2\text{-}\eta^2\text{-}C{\equiv}CPh)(\mu\text{-dppe})$ (**5A**).

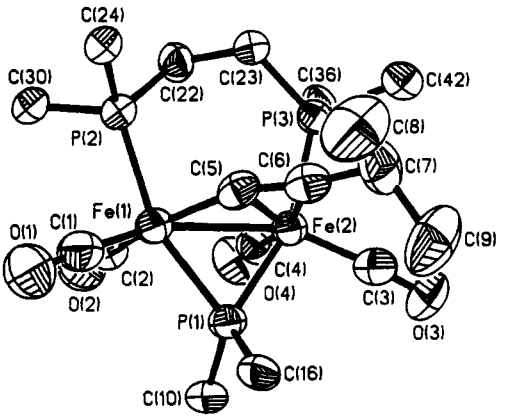


**Figure 4.** ORTEP plot of the molecular structure of $Fe_2(CO)_4(\mu\text{-}PPh_2)(\mu_2\text{-}\eta^2\text{-}C{\equiv}CPr^i)(\mu\text{-dppe})$ (**5B**).

metal bond and trans to the acetylide. However, since the acetylide is $\sigma$–$\pi$ bound, each metal atom should have a unique set of carbonyl ligands. In the $^{31}P\{^1H\}$ NMR spectra of **4A–C** and **5A–C** the two dppm or dppe phosphorus atoms are equivalent, even though one is attached to the Fe atom $\sigma$-bound to the acetylide, and the other to the Fe atom $\pi$-bound the hydrocarbyl. In the $^1H$ NMR spectra of the isopropyl CO substitution products **4B** and **5B** only one isopropyl methyl resonance is present. A single $^{13}C$ resonance for the isopropyl methyl groups is also observed in the $^{13}C\{^1H\}$ NMR spectra of these compounds, even though the two methyl groups are diastereotopic, as illustrated in the structure of **5B** (Figure 4). This implies that a dynamic process must be equilibrating the two metal sites in the molecule. A "windshield-wiper" motion

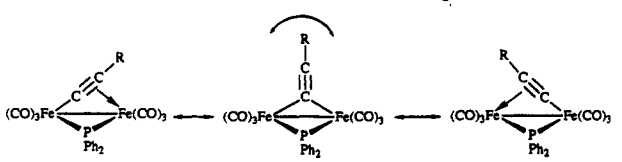

**Table VIII.** $^{13}C\{^1H\}$ NMR $C_\alpha$ and $C_\beta$ Resonances for Compounds 4A–C and 5A–C

| compd | R | $\delta(C_\alpha)$, ppm | $^2J_{PC}$, Hz | $^2J_{PC'}$, Hz | $\delta(C_\beta)$, ppm | $^3J_{PC}$, Hz |
|---|---|---|---|---|---|---|
| | | | $\mu$-dppm | | | |
| **4A** | Ph | 83.5 | 38.0 | | 100.0 | 9.5 |
| **4B** | $Pr^i$ | 108.8 | 60.9 | 11.7 | 107.0 | 9.4 |
| **4C** | $Bu^t$ | 107.6 | 53.9 | 11.1 | 110.1 | 7.5 |
| | | | $\mu$-dppe | | | |
| **5A** | Ph | 83.5 | 38.0 | | 101.8 | 9.8 |
| **5B** | $Pr^i$ | 114.2 | 66.8 | 17.6 | 107.0 | 8.7 |
| **5C** | $Bu^t$ | 112.6 | 51.9 | 19.9 | 114.3 | 8.4 |

of the acetylide, similar to that in the parent complexes, **1A–C**, and observed for other acetylide compounds,[7,8,17] is likely responsible for the dynamic behavior. Variable-temperature $^{31}P\{^1H\}$ NMR studies were carried out on **4A** and **5A** in order to confirm this phenomenon. Figure 3 illustrates typical spectra for **5A**.

For **4A** at room temperature the phosphido bridge resonance at 178.4 ppm is a triplet ($^2J_{PP}$ = 114.3 Hz) and the dppm resonance is a doublet ($\delta$ 58.6 ppm, $^2J_{PP}$ = 114.3 Hz). At −85 °C the fluxionality of the $\sigma$–$\pi$ acetylide is frozen out, resulting in an ABX type spectrum. The phosphido bridge resonance becomes a doublet of doublets at 180.2 ppm ($^2J_{PP}$ = 134.4 Hz, $^2J_{PP'}$ = 90.0 Hz), with the dppm resonances at 60.6 ppm ($^2J_{PMP}$ = 139.4 Hz, $^2J_{PCP}$ = 64.5 Hz) and 58.4 ppm ($^2J_{PMP}$ = 90.0 Hz, $^2J_{PCP}$ = 64.5 Hz). From the coalescence temperature at −63 °C, $\Delta G$ for the $\sigma$–$\pi$ acetylide fluxionality[18] was estimated at 10 kcal mol$^{-1}$, which is at the low end of the range of values (19.05–10.0 kcal mol$^{-1}$) measured for $\mu_2$-$\eta^2$-acetylide fluxionality.[7,8,17]

The $^{13}C$ acetylide resonances for compounds **4A–C** and **5A–C** lie in the range 114.2–83.5 ppm (Table VIII), within the region expected for the $\mu_2$-$\eta^2$-acetylides (110–65 ppm).[20] In the parent $Fe_2(CO)_6(\mu\text{-}PPh_2)(\mu_2\text{-}\eta^2\text{-}C{\equiv}CR)$ complexes the $C_\alpha$ resonance is downfield of $C_\beta$ for R = Ph but upfield of $C_\beta$ for R = $Pr^i$ and $Bu^t$. This trend is reversed for the bridging diphosphine compounds **4A–C** and **5A–C**. The resonance for $C_\beta$ is a doublet with a small coupling to the phosphido bridge phosphorus atom (7.5–9.5 Hz), as is found in the parent compound. The resonances for $C_\alpha$ are strongly coupled to the phosphido bridge phosphorus atom ($^2J_{PP}$ = 38–66.5 Hz), as in the unsubstituted acetylides, and weakly coupled to only one of the bridging diphosphine phosphorus atoms, presumably at the $\sigma$-bonded acetylide end, Fe(1) ($^2J_{PC}$ = 10–19.9 Hz).

In **4A–C** the dppm $CH_2$ group gives a $^{13}C$ resonance within the range 31.2–41.3 ppm as a triplet ($^1J_{PC}$ = 19.8–25.0 Hz) while in the dppe-bridged complexes, **5A–C**, the $CH_2$ resonance is a doublet at room temperature at approximately 21 ppm ($^1J_{PC}$ = 22 Hz).

The spectral features of **2A** differ markedly from those of **4A–C** and **5A–C**, as might be expected from its unusual structure. In the $^{31}P\{^1H\}$ NMR spectrum, the phosphido bridge resonance moves upfield from that in the starting material to 112.6 ppm. The metal-bound dppm phosphorus resonance is a doublet coupled to the C-bound

(17) (a) Lee, K.; Pennington, W. T.; Cordes, A. W.; Brown, T. L. *J. Am. Chem. Soc.* **1985**, *107*, 631. (b) Mercer, R. J.; Green, M.; Orpen, A. G. *J. Chem. Soc., Chem. Commun.* **1986**, 567. (c) Ten Hoedt, R. W. M.; Van Koten, G.; Noltes, J. G. *J. Organomet. Chem.* **1977**, *133*, 173. (d) Ten Hoedt, R. W. N.; Noltes, J. G.; Van Koten, G.; Spek, A. L. *J. Chem. Soc., Dalton Trans.* **1978**, 1800. (e) Koridze, A. A.; Kizas, O. A.; Kolobora, N. E.; Petrovski, P. V. *Bull. Acad. Sci. USSR, Div. Chem. Sci. (Engl. Transl.)* **1984**, *33*, 437.

(18) Binsch, G. *Topics in Stereochemistry*; Interscience Publishers: New York, 1988; Vol. 3, p 97.

(19) Carty, A. J.; Cherkas, A. A.; Randall, L. H. *Polyhedron* **1988**, *7*, 1045.

(20) Bruce, M. I. *Chem. Rev.* **1991**, *91*, 197.

dppm phosphorus atom but not the phosphido bridge phosphorus atom at 54.3 ppm ($^2J_{PCP}$ = 18.1 Hz). The lack of coupling to the phosphido bridge is indicative of coordination cis to the phosphido bridge. The phosphorus atom bound to the acetylide carbon atom gives a resonance at 5.9 ppm ($^2J_{PCP}$ = 18.1 Hz, $^4J_{PP}$ = 11.8 Hz).

In the $^{13}C\{^1H\}$ NMR spectrum, a signal at 297.2 ppm is indicative of a $\mu_2$-vinylidene carbon atom.[20] This resonance is a doublet of doublets of doublets but appears as a doublet of triplets as a result of the accidental equivalence of two of the coupling constants ($^2J_{PC}$ = 76.6 Hz, $^2J_{PC'}$ = $^3J_{PC}$ = 11.3 Hz).

There are three resonances due to the carbonyl carbon atoms. Two can be assigned to the two carbonyl groups attached to the dppm-bound Fe, at 220.3 ppm (ddd, $^2J_{PC}$ = 16.6 Hz, $^2J_{PC'}$ = 4.4 Hz, $^4J_{PC}$ < 1 Hz) and at 218.9 ppm (dd, $^2J_{PC}$ = 15.1 Hz, $^2J_{PC}$ = 7.9 Hz), while the three carbonyl groups on the other iron atom are made equivalent, probably through trigonal rotation, and give a signal at 216.5 ppm (d, $^2J_{PC}$ = 2.6 Hz). The resonance of $C_\beta$ is a doublet ($^1J_{PC}$ = 81.7 Hz) at 114.1 ppm, which is upfield of the normal $Fe_2$ vinylidene range (125.4–153.6 ppm), and the dppm $CH_2$ gives a peak at 24.7 ppm (dd, $^1J_{PC}$ = 67.6 Hz, $^1J_{PC'}$ = 12.4 Hz).

The $^1H$ NMR spectrum of **1** shows that the methylene protons belonging to the dppm ligand are nonequivalent with resonances at 3.45 and 2.28 ppm.

**C. Structures of 2A and 5B.** Although the spectroscopic features of **2** were consistent with the presence of a $\mu_2$-vinylidene ligand, an alternative structure was that of a five-membered ring system formed via attack at $C_\alpha$ and formation of a two-carbon bridge (see structure V).

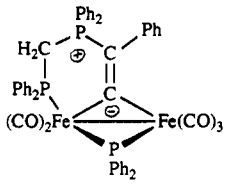


2A

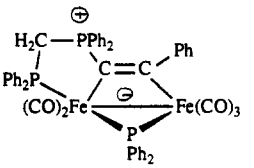


V

To verify the structure of **2A** a single-crystal X-ray structure analysis was carried out. A perspective view of the structure together with the atomic numbering is illustrated in Figure 2. The principal structural feature within the binuclear molecule is a short Fe(1)–Fe(2) bond (2.5683 (8) Å) bridged by a diphenyl phosphido group and by the carbon atom C(7) of the novel vinylidene ligand. The $\beta$-carbon atom of the $\mu$-vinylidene (C(8)) is attached to one phosphorus atom of a dppm ligand bridging this carbon atom and the iron atom Fe(1). The atoms Fe(1), C(7), C(8), P(3), C(16), and P(2) thus form a six-membered unsaturated ring system. Since the P(3) atom is attached to four carbon atoms, it is a phosphonium center and the complex is zwitterionic with the negative charge delocalized onto the $Fe_2(CO)_5(\mu\text{-}PPh_2)$ core.

The structural features of the $\mu$-vinylidene ligand compare well with the parameters established for other vinylidenes. Thus the Fe(1)–C(7) (1.938 (4) Å) and Fe(2)–C(7) (1.949 (4) Å) bond lengths are well within the range of iron–carbon distances in $Fe_2$ vinylidene complexes (1.874 (3)–1.969 (7) Å)[20] and the C(7)–C(8) bond length (1.346 (5) Å) is typical of C=C bond distances in diiron $\mu_2$-vinylidenes (1.266 (6)–1.358 (5) Å)[20] and close to the accepted $C_{sp^2}$–$C_{sp^2}$ bond length of 1.34 Å.[21] The P(3)–C(8) bond length of 1.765 (4) Å is similar to the P=C bond distances of 1.68–1.72 Å found in phosphaalkenes and is indicative of partial double-bond character. This multiple bonding indicates that the P(3)–C(8)–C(7)–Fe(2) bond system is partially delocalized with contributing resonance structures III and IV.

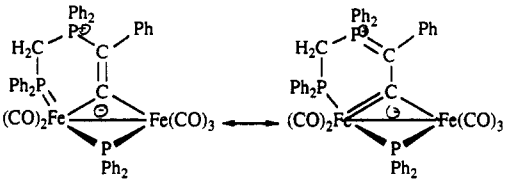


III IV

Contributing resonance structures to delocalised bonding in **2**

The P(2)–Fe(1) bond length is 2.178 (1) Å. When compared with the phosphido bridge–iron bond lengths P(1)–Fe(1) = 2.204 (1) Å and P(1)–Fe(2) = 2.225 (1) Å or the P(2)–Fe(1) and P(3)–Fe(2) bond lengths of 2.211 (2) and 2.257 (2) Å in **5**, it would appear that the P(2)–Fe(1) bond is also shortened by delocalization in the six-membered ring. The Fe(1)–Fe(2) bond length of 2.5683 (8) Å is shorter than that found in the starting material $Fe_2(CO)_6(\mu\text{-}PPh_2)(\mu_2\text{-}\eta^2\text{-}C{\equiv}CPh)$ (2.597 (2) Å)[23] but typical of diiron vinylidenes (2.428 (1)–2.674 (1) Å).[20]

Further evidence of the $sp^2$ nature of the C(8) carbon atom comes from the angles around C(8). The P(3)–C(8)–C(19) angle is 116.5 (2)°, the P(3)–C(8)–C(7) angle is 117.5 (2)°, and the C(7)–C(8)–C(9) angle is 126.0 (2)°, close to the 120° angle expected for an $sp^2$ carbon atom. The C(17) atom, although formally $sp^2$, has a severely distorted stereochemistry since the Fe(1)–C(17)–Fe(2) angle is 82.71 (2)°. To compensate, the Fe(1)–C(7)–C(8) and Fe(2)–C(7)–C(8) angles are expanded beyond 120° to 139.9 (2) and 136.9 (2)°, respectively. The Fe(1)–Fe(2)–C(7)–C(8)–P(3) and C(9) atoms lie essentially in one plane. Examples of diphosphine ligands "coordinated" to one carbon atom of a hydrocarbyl and a metal atom are rare. In this respect it is interesting to note that the only other example is also a zwitterionic diiron complex, namely $Fe_2(CO)_5(\mu\text{-}CO)[\mu\text{-}C(=CH_2)Ph_2PCH_2PPh_2]$,[6] although in this case the dppm ligand forms part of a five-membered ring, the dimetal center being bridged by a two-carbon ligand. In this case the bond length from the cationic ylide phosphorus atom to the bridging carbon is also shortened, as expected (1.755 (8) Å), being close to the corresponding value of 1.765 (4) Å found in **2A**.

The structure of **5B** was confirmed by a single-crystal X-ray analysis (Figure 4). As expected from the spectroscopic data, the dppe ligand bridges the two iron centers to form a six-membered ring. The two dppe phosphorus atoms are both trans to the phosphido bridge, as predicted from the large $^{31}P$–$^{31}P$ coupling constant (118 Hz). The acetylide is $\sigma$-bound to Fe(1) and $\pi$-bound to Fe(2), giving asymmetry to the molecule in the solid state. However, the molecule exhibits a dynamic motion of the acetylide as described above. The pseudo plane of symmetry bisects the Fe(1)–Fe(2) and C(22)–C(23) bonds through the phosphido bridge phosphorus atom.

Although the R group on the acetylide in **5B** is isopropyl, the Fe(1)–Fe(2)–P(1)–C(5)–C(6) core is similar to that in the unsubstituted diiron complex $Fe_2(CO)_6(\mu\text{-}PPh_2)(\mu_2\text{-}\eta^2\text{-}C{\equiv}CPh)$[23] and the monosubstituted complex $Fe_2(CO)_5(\mu\text{-}PPh_2)(\mu_2\text{-}\eta^2\text{-}C{\equiv}CPh)(PPh_3)$[24] where the acetylide

(21) Bent, H. A. *Chem. Rev.* **1961**, *61*, 275.
(22) Knoll, K.; Huttner, G.; Wasiucionek, M.; Zsolnai, L. *Angew. Chem., Int. Ed. Engl.* **1984**, *23*, 739.
(23) Patel, H. A.; Fischer, R. G.; Carty, A. J.; Naik, D. V.; Palenik, G. J. *J. Organomet. Chem.* **1973**, *60*, C49.
(24) Smith, W. F.; Yule, J.; Taylor, N. J.; Paik, H. N.; Carty, A. J. *Inorg. Chem.* **1977**, *16*, 1593.

R group is phenyl. The presence of the bridging dppe causes a slight expansion of the $Fe_2C_2$ portion of the core from the unsubstituted complex, the Fe–Fe bond distance increasing to 2.622 (1) Å in **5B** from 2.597 (2) Å and the C≡C bond distance increasing slightly from 1.232 (10) to 1.261 (11) Å in **2A**. The Fe(1)–$C_\alpha$ bond length also increases to 2.126 (7) Å in **5B** from 1.891 (6) Å, and the acetylide bend back-angle, $C_\alpha$–$C_\beta$–$C_R$ is more acute in **5B** (159.8 (5) vs 162.3 (8)°) than in **2A**.

In the monosubstituted complex, $Fe_2(CO)_5(\mu\text{-}PPh_2)(\mu_2\text{-}\eta^2\text{-}C{\equiv}CPh)(PPh_3)$, the phosphine is bound to Fe(1), which has the σ-bound acetylide atom. The phosphine is in a position trans to the phosphido bridge with an Fe(1)–P(2) distance of 2.274 (1) Å. In **5B** the dppe phosphorus atoms are also trans to the phosphido bridge, with slightly shorter Fe–P bond lengths, Fe(1)–P(2) = 2.211 (2) Å and Fe(2)–P(3) = 2.257 (2) Å.

## Conclusion

In summary these results provide a rather nice illustration of the fact that in hydrocarbyl complexes where the unsaturated complex is highly activated to nucleophilic attack, by $\sigma$–$\pi$ coordination, phosphorus ligands, even bidentate ones with a high affinity for bridging (dppm) or chelating (dppe) metal centers, may preferentially attack an activated carbon atom, leading initially to a phosphonium zwitterion. Although at first sight it might appear unusual that ligands normally associated with CO substitution should preferentially "coordinate" to carbon, site selectivity in these nucleophilic reactions is, at least in part, orbitally controlled and the LUMO may be principally located on a hydrocarbyl carbon atom. Only when this site is sterically inaccessible will CO substitution become dominant.

**Acknowledgment.** We are grateful to the Natural Sciences and Engineering Research Council of Canada for grants (to A.J.C.) and scholarships (to A.A.C., L.H.R., and S.M.B.) in support of this work. A NATO/SERC postdoctoral fellowship to G.H. is also gratefully acknowledged.

**Registry No.** **1A**, 52970-25-9; **1B**, 62475-91-6; **1C**, 59584-68-8; **2A**, 139198-79-1; **2A′**, 139198-89-3; **2B**, 139198-83-7; **2B″**, 139198-91-7; **2C″**, 139198-93-9; **3A**, 139198-80-4; **3A′**, 139198-90-6; **3B**, 139198-84-8; **3B″**, 139198-92-8; **3C″**, 139198-94-0; **4A**, 139198-81-5; **4B**, 139198-85-9; **4C**, 139198-88-2; **5A**, 139198-82-6; **5B**, 139198-87-1; **5C**, 139242-49-2.

**Supplementary Material Available:** For both structural analyses, tables of anisotropic thermal coefficients (Tables S1 and S2), the remaining bond distances and angles (Tables S3 and S4), and hydrogen atom and solvent molecule atomic coordinates (Tables S5 and S6) (10 pages); listings of structure factors (Tables S7 and S8) (49 pages). Ordering information is given on any current masthead page.

# Thiolate-Bridged Dichromium Complexes. Syntheses and Crystal Structures of $[CpCr(CO)_2(SPh)]_2$ and $[CpCr(SPh)]_2S$

Lai Yoong Goh* and Meng S. Tay

*Department of Chemistry, University of Malaya, 59100 Kuala Lumpur, Malaysia*

Thomas C. W. Mak* and Ru-Ji Wang

*Department of Chemistry, The Chinese University of Hong Kong, Shatin, NT, Hong Kong*

*Received August 6, 1991*

The predominant product obtained from the reaction of $[CpCr(CO)_3]_2$ with $Ph_2S_2$ varied with reaction temperature as follows: $[CpCr(CO)_2(SPh)]_2$ (**3**), 32.9%, ambient temperature; $[CpCr(CO)(SPh)]_2$ (**4**), 53.07%, 60 °C; $[CpCr(SPh)]_2S$ (**5**), 20.7%, 80 °C. A thermolysis study showed the degradation of **3** and **4** to **5** and eventually to $Cp_4Cr_4S_4$. The thiolate-bridged complexes have been characterized by elemental and spectral analyses. **3** and **5** have also been structurally determined. Crystal data: **3**, monoclinic, space group $P2_1/c$ (No. 14), $a$ = 9.138 (2) Å, $b$ = 14.195 (6) Å, $c$ = 18.879 (5) Å, $\beta$ = 101.77 (2)°, $V$ = 2397 (1) Å$^3$, $Z$ = 4; **5**, triclinic, space group $P\bar{1}$ (No. 2), $a$ = 9.548 (1) Å, $b$ = 10.122 (2) Å, $c$ = 13.003 (1) Å, $\alpha$ = 103.71 (1)°, $\beta$ = 100.351 (9)°, $\gamma$ = 98.62 (1)°, $V$ = 1176.4 (3) Å$^3$, $Z$ = 1.

## Introduction

Transition-metal complexes containing thiolate ligands have commanded a long standing interest on account of their relevance to biological[1] and catalytic[2] processes. The main interest has been concentrated on Fe, Mo, and W. Among the earliest examples of alkyl mercapto complexes were those of Fe[3] and Mo,[4] which date back to the 1960s. A commonly used synthetic route has involved the reaction of transition-metal carbonyl complexes with organic sulfides or disulfides under varying reaction conditions. Thus the reaction $[CpMo(CO)_3]_2$ with $R_2S_2$ led to the isolation of $[CpMo(SR)_2]_n$ (R = Me, $n$ = 2;[4a] and R = Ph, $n$ = $x$)[4b] under reflux conditions in methylcyclohexane (101 °C) and

(1) See for example: (a) Newton, W. E. In *Sulfur, Its Significance for Chemistry, for the Geo-, Bio-, and Cosmosphere and Technology*; Müller, M., Krebs, B., Eds.; Studies in Inorganic Chemistry; Elsevier: Amsterdam, 1984; Vol. 5, p 409. (b) Holm, R. H. *Chem. Soc. Rev.* **1981**, *10*, 455. (c) Arber, J. M.; Dobson, B. R.; Eady, R. R.; Stevens, P.; Hasnain, S. S.; Garner, C. D.; Smith, B. E. *Nature* **1987**, *325*, 372. (d) Berg, J. M.; Holm, R. H. In *Metal Ions in Biology*; Spiro, T. G., Ed.; Wiley: New York, 1982; Vol. 4, Chapter 1. (e) Vergamini, P. T.; Kubas, G. J. *Prog. Inorg. Chem.* **1977**, *21*, 261.

(2) See for example: (a) Weisser, O.; Landa, S. *Sulfide Catalysts; Their Properties and Applications*; Pergamon Press: New York, 1973. (b) Dilworth, J. R. In ref 1a, p 141. (c) Wedd, A. G. In ref 1a, p 181. (d) Vahrenkamp, H. *Angew. Chem., Int. Ed. Engl.* **1975**, *14*, 322. (e) Blower, P. J.; Dilworth, J. R. *Coord. Chem. Rev.* **1987**, *76*, 121.

(3) (a) King, R. B.; Treichel, P. M.; Stone, F. G. A. *J. Am. Chem. Soc.* **1961**, *83*, 3600. (b) King, R. B. *J. Am. Chem. Soc.* **1962**, *84*, 2460. (c) King, R. B.; Bisnette, M. B. *J. Am. Chem. Soc.* **1964**, *86*, 1267. (d) Ahmad, M.; Bruce, R.; Knox, G. R. *J. Organomet. Chem.* **1966**, *6*, 1.

(4) (a) King, R. B. *J. Am. Chem. Soc.* **1963**, *85*, 1587. (b) Tilley, E. W.; Schermer, E. D.; Baddley, W. H. *Inorg. Chem.* **1968**, *7*, 1925. (c) King, R. B.; Bisnette, M. B. *Inorg. Chem.* **1965**, *4*, 482. (d) Treichel, P. M.; Wilkes, G. R. *Inorg. Chem.* **1966**, *5*, 1182.

0276-7333/92/2311-1711$03.00/0 